Electronic Supplementary Information

(Chemical Communications)

Taxodisones A and B: bioactive C_{30}-terpenes with new skeletons from *Taxodium distichum* and their biosynthetic origin

Wen-Li Wang,[a] Xiao-Qin Liu,[a] Mei-Hui Zhang,[a] Bin Lin,[b] Dong-Rong Zhu,[a] Ling-Nan Li,[a] Chen Chen,[a] Chao Han,[a] Jian-Guang Luo,[*a] and Ling-Yi Kong[*a]

[a] Jiangsu Key Laboratory of Bioactive Natural Product Research and State Key Laboratory of Natural Medicines, School of Traditional Chinese Pharmacy, China Pharmaceutical University, 24 Tong Jia Xiang, Nanjing 210009, People's Republic of China. cpu_lykong@126.com

[b] School of Pharmaceutical Engineering, Shenyang Pharmaceutical University, 103 Wenhua Road, Shenyang 110016, China

Table of Contents

1. The details of structure elucidations of compounds 1 and 2

Taxodisone A (**1**) was obtained as colorless needle crystals (MeOH/CH_2Cl_2, 1:3). Its molecular formula $C_{30}H_{42}O_3$ was determined from the HRESIMS (*m/z* 473.3029 $[M+Na]^+$, calcd 473.3026) and ^{13}C NMR data (Table S1), suggesting ten degrees of unsaturation. The IR absorptions at 3357, 1711, and 1640 cm^{-1} indicated the presence of hydroxyl, carbonyl, and alkenyl groups, respectively. The ^1H NMR spectrum of **1** displayed resonances for five singlet methyls (δ_H 0.98, 1.26, 1.27, 1.58, and 1.66), two doublet methyls [δ_H 1.07 (d, J = 7.0 Hz) and 1.09 (d, J = 7.0 Hz)], and three olefinic protons [δ_H 6.80 (s), 5.58 (br d, J = 5.7 Hz), and 5.04 (t, J = 6.6 Hz)] (Table S1). The ^{13}C NMR spectrum with the aid of HSQC and DEPT spectra exhibited 30 carbon signals, including seven methyls, seven methylenes, six methines (three olefinic at δ_C 148.8, 123.5, and 119.7) and ten quaternary carbons (two carbonyls at δ_C 211.5 and 181.7 and five olefinic carbons at δ_C 144.0, 139.0, 138.4, 134.9, and 132.3). Apart from six degrees of unsaturation occupied by two ketone carbonyls and four double bonds, a tetracyclic structure was required for **1** to fulfill the demand of the unsaturation.

Construction of the detailed planar structure of **1** was assembled by interpretation of 2D NMR data. The ABC ring system was assigned by key HMBC correlations (Fig. 1A) from H_3-20 to C-1, C-5, C-9, and C-10; from H_3-19 and H_3-18 to C-3, C-4, and C-5; from H_3-16 and H_3-17 to C-13 and C-15, and from H-15 to C-13, C-14, C-16, and C-17, coupling with the ^1H–^1H COSY cross-peaks from H_2-1 via H_2-2 to H_2-3. Furthermore, the key ^1H–^1H COSY cross-peak H-7 to H_2-1′, with the key HMBC correlations from H_2-10′ to C-7, C-8, and C-14; from H-2′ to C-7; from H_2-1′ to C-6, C-7, and C-8; from H-7 to C-1′, C-2′, and C-10′ revealed a six-membered ring (D).

By the HMBC cross-peaks of H_3-9′ and C-6′, C-7′, and C-8′; H_3-8′ and C-6′, C-7′, and C-9′; H-6′ and C-4′, and C-8′; H-2′ and C-4′, combined with the ^1H–^1H COSY correlations of H_2-4′/H_2-5′, H_2-5′/H-6′ revealed the presence of the side chain was assigned at C-3′. Therefore, the planar structure of **1** was established.

The relative configuration of **1** was assigned by the ROESY spectrum. The typical ROESY correlations of H-5/H_3-18, and H-5/H_2-10′ indicated that they were cofacial and defined to be *α*-orientated, while the correlations of H_3-19 with H_3-20, and H_3-20 and H-7 revealed that these protons were on the same side with *β*-orientations (Fig. 2B). In addition, the double bond between C-2′ and C-3′ of **1** was deduced as a *Z*-configuration by the clear ROESY correlation of H-2′/H-4′.

After many solvent system attempts, a high-quality crystal of compound **1** was obtained in MeOH/CH_2Cl_2 (1:3), and then **1** was subjected to single-crystal X-ray diffraction with a Cu K*α* radiation (Fig. 3). Therefore, the structure of **1** was further confirmed and the absolute configuration was determined as 5*S*, 7*S*, 8*S*, 10*S* with the Flack parameter of 0.05 (6).[1]

Taxodisone B (**2**) possessed the same molecular formula of $C_{30}H_{42}O_3$ as **1** based on the HRESIMS ion peak at *m/z* 473.3029 $[M+Na]^+$ (calcd 473.3026) and the ^{13}C NMR spectrum. The 1D and 2D NMR data of **2** were highly similar to those of **1**. The main difference was the linkage pattern of rings B and D. The key HMBC correlations from H-7 to C-3′, and C-10′; from H_2-1′ to C-8 and C-14; from H-10′ to C-6 and C-7, together with the $^1H-^1H$ COSY cross-peak of H-7/H_2-10′, suggested the linkage of C-7–C-10′ and C-8–C-1′ (Fig. S1). This deduction was further confirmed by the ROESY cross-peaks of H_3-18/H-5, and H-5/H_2-1′ (Fig. S1). The structure and absolute configuration (5*S*, 7*S*, 8*S*, 10*S*) of **2** was finally consolidated using single crystal X-ray diffraction (Fig. S2) [Cu Kα radiation, a Flack parameter, 0.10(8)].[3]

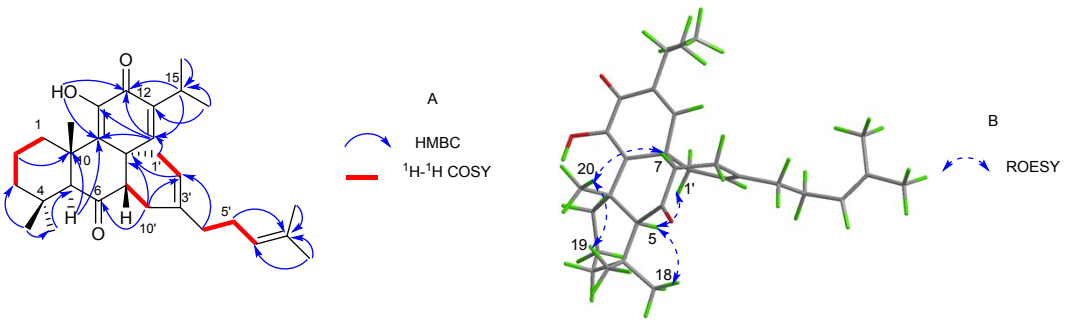

Figure S1 Key ^{1}H-^{1}H COSY, HMBC, and ROESY correlations of compound **2**.

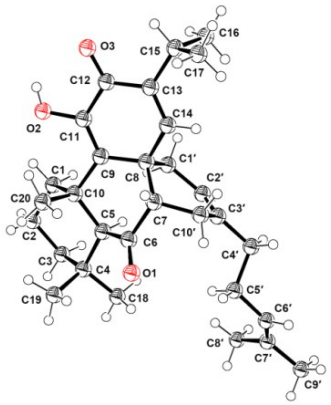

Figure S2 ORTEP drawing of **2**.

Table S1 The ^{1}H (500 MHz) and ^{13}C NMR (125 MHz) data of compounds **1** and **2** in $CDCl_3$.

No.	**1**		**2**	
	δ_H (J in Hz)	δ_C	δ_H (J in Hz)	δ_C
1	2.94, m; 1.46, m	35.9	2.91, m; 1.44, m	35.8
2	1.70, m; 1.54, m	19.0	1.73, m; 1.54, m	19.0
3	1.41, m; 1.13, m	42.9	1.39, m; 1.10, m	42.8
4		32.6		32.6
5	2.68, s	60.6	2.74, s	60.3
6		211.5		211.4
7	1.99, overlapped	45.5	2.03, overlapped	45.9
8		40.6		39.7
9		139.0		139.0
10		41.5		41.4
11	7.09, s	144.0	7.01, s	144.0
12		181.7		181.7
13		138.4		138.2
14	6.80, s	148.8	6.81, s	148.8
15	2.95, sept (7.0)	26.8	2.93, sept (7.0)	26.8
16	1.07, d (7.0)	21.7	1.07, d (7.0)	21.6
17	1.09, d (7.0)	21.6	1.09, d (7.0)	21.9
18	0.98, s	33.7	0.98, s	33.6
19	1.26, s	22.3	1.26, s	22.3
20	1.27, s	20.2	1.27, s	20.2
1′	2.78, dd (5.7, 18.2); 2.50, m	26.1	3.01, d (19.9); 1.94, d (19.9)	33.7
2′	5.58, br d (5.7)	119.7	5.44, br s	118.0
3′		134.9		136.6
4′	2.03, m; 2.01, m	37.6	2.08, overlapped; 2.05, overlapped	38.0
5′	2.07, m; 1.67, m	26.5	2.13, m; 2.04, overlapped	26.3
6′	5.04, t (6.6)	123.5	5.06, *t*-like	123.7
7′		132.3		132.1
8′	1.66, s	25.8	1.67, s	25.8
9′	1.58, s	17.9	1.61, s	17.9
10′	2.93, overlapped; 1.79, d (19.5)	36.2	2.67, d (17.8); 1.41, m	28.6

1 H. D. Flack, *Acta Cryst.*, 1983, **A39**, 876-881.

2. General experimental procedures

UV spectra were measured by a Shimadzu UV-2450 spectrometer (Shimadzu, Tokyo, Japan). ECD spectra were measured by a JASCO 810 spectropolarimeter (JASCO, Tokyo, Japan). A JASCO-P1020 polarimeter was used to record optical rotation values. A Tensor 27 infrared spectrometer (Bruker) was used to record the IR spectra using KBr disks. All the NMR spectra were recorded on Bruker Avance-500 and Ascend-600 instruments in $CDCl_3$ and the internal standard was TMS. An Agilent 6520B Q-TOF mass instrument was employed to acquire HRESIMS spectra. Silica gel (200-300 mesh) was obtained from Qingdao Marine Chemical Plant (Qingdao, P. R. China). Sephadex LH-20 was obtained from Pharmacia Company. A Shimadzu LC-6AD series instrument equipped with a Shim-pack RP-C18 (20 mm × 250 mm, 5 μm) and a Shimadzu SPD-20A detector was employed to conduct preparative RP-HPLC analysis. A JASCO LC-Net II/ADC equipped with a JASCO PU-2089 Plus Quaternar Gradient Pump and a CD-2095 Plus Chiral Detector was employed to conduct NP-HPLC with a CHIRALPAK AD-H (10 mm × 250 mm, 5 μm).

2.1. Plant material

In March 2018, plants materials (seeds of *T. distichum*) were obtained from Shanghai, China. A voucher specimen (No. TD201803) was stored in the Department of Natural Medicinal Chemistry, China Pharmaceutical University.

2.2. Extraction and isolation

The powdered seeds of *T. distichum* (5.0 kg) were extracted with EtOH/H_2O (95/5) (3 × 10 L, each 2 h), followed by concentration process under vacuum pressure. The extract (0.8 kg) was solved in 1.0 L water (60 °C) and extracted with EtOAc (3 × 1.0 L). The obtained EtOAc extract (200 g) was loaded onto silica gel chromatographic column (CC), and fractions (1-3) were acquired through elution with a petroleum

ether/EtOAc gradient system (100:0, 100:100 and 0:100). Fr.2 (50 g) was isolated by the ODS column eluted with MeOH/H_2O gradient system (50:50-100:0) to afforded fractions A-E. Fraction D (5.0 g) was isolated by ODS CC (MeOH/H_2O, 80:20-100:0) to afford six subfractions (D1-D6). Compound **3** (230.0 mg) was afforded from D2 by recrystallization. Fraction E (0.5 g) was loaded onto ODS CC and eluted by MeOH to obtain five subfractions (E1-E5). Compounds **1** (t_R = 44.6 min, 10.0 mg) and **2** (t_R = 36.5 min, 8.0 mg) were obtained from subfraction E5 by NP-HPLC CC (*n*-hexane:isopropanol = 98:2, 1.0 mL/min).

2.3. Structural characterizations of compounds 1 and 2

Taxodisone A (**1**)

Colorless needle crystals (MeOH/CH_2Cl_2, 1:3); $[\alpha]_D^{25}$ 146.0 (*c* 0.04, MeOH); UV (MeOH) λ_{max} (log ε) 205 (14.98), 254 (5.46) nm; IR ν_{max} 3357, 2926, 2867, 1711, 1641, 1610, 1371 cm^{-1}; ^1H and ^{13}C NMR ($CDCl_3$), see Table S1; HRESIMS *m/z* 473.3023 $[M+Na]^+$ (calcd for $C_{30}H_{42}NaO_3$, 473.3026).

Taxodisone B (**2**)

Colorless needle crystals (isopropanol); $[\alpha]_D^{25}$ 120.2 (*c* 0.05, MeOH); UV (MeOH) λ_{max} (log ε) 205 (6.50), 253 (3.14) nm; IR ν_{max} 3357, 2926, 2867, 1711, 1641, 1610, 1371 cm^{-1}; ^1H and ^{13}C NMR ($CDCl_3$), see Table S1; HRESIMS *m/z* 473.3029 $[M+Na]^+$ (calcd for $C_{30}H_{42}NaO_3$, 473.3026).

2.4. X-ray crystallographic analysis

Colorless needle crystals of **1** were obtained from MeOH:CH_2Cl_2 = 1:3. A suitable crystal was selected and subjected on a Bruker APEX-II CCD diffractometer. The crystal was kept at 298 K during data collection. Using Olex2,[1] the structure was solved with the ShelXT[2] structure solution program using Intrinsic Phasing and refined with the ShelXL[3] refinement package using Least Squares minimisation. Crystal data for compound **1**: $C_{30}H_{42}O_3$, (M = 450.63 g/mol), orthorhombic, space group $P2_12_12_1$ (no.

19), a = 7.6085(10) Å, b = 18.276(3) Å, c = 18.693(2) Å, V = 2599.4(6) Å^3, Z = 4, T = 298 K, μ (Cu Kα) = 0.560 mm^{-1}, *Dcalc* = 1.152 g/cm^3, 43496 reflections measured (6.764° ≤ 2Θ ≤ 149.674°), 5309 unique (R_{int} = 0.0380, R_{sigma} = 0.0193) which were used in all calculations. The final R_1 was 0.0316 (I > 2σ(I)) and wR_2 was 0.0870 (all data). Flack parameter 0.05 (6).

Colorless square crystals of compound **2** were obtained from isopropanol. A suitable crystal was selected and obtained on a Bruker APEX-II CCD diffractometer. The crystal was kept at 100.0 K during data collection. Using Olex2,[1] the structure was solved with the ShelXT[2] structure solution program using Intrinsic Phasing and refined with the ShelXL[3] refinement package using Least Squares minimisation. Crystal data for **2**: $C_{30}H_{42}O_3$ (M = 450.63 g/mol), monoclinic, space group $P2_1$ (no. 4), a = 10.2640(3) Å, b = 12.5469(3) Å, c = 20.5284(5) Å, β = 101.8070(10)°, V = 2587.74(12) Å^3, Z = 4, T = 100.0 K, μ(CuKα) = 0.562 mm^{-1}, *Dcalc* = 1.157 g/cm^3, 35509 reflections measured (4.398° ≤ 2Θ ≤ 145.392°), 9039 unique (R_{int} = 0.0402, R_{sigma} = 0.0360) which were used in all calculations. The final R_1 was 0.0333 (I > 2σ(I)) and wR_2 was 0.0920 (all data). Flack parameter 0.10 (8).

Crystallographic data for **1** and **2** have been deposited in the Cambridge Crystallographic Data Center (deposition number: CCDC 1935880, 1935884). Copies of the data can be obtained free of charge via www.ccdc.cam.ac.uk/conts/retrieving.html or from the Cambridge Crystallographic Data Centre, 12, Union Road, Cambridge CB2 1EZ, U.K. [fax (+44)1223-336-033; or e-mail: deposit@ccdc.cam.ac.uk].

1. Oleg VD, Luc JB, Richard JG, Judith AKH, Horst P. OLEX2: a complete structure solution, refinement and analysis program. *J Appl Crystallogr* 2009;**42**:339-341.
2. Sheldrick GM. SHELXT-integrated space-group and crystal-structure determination. *Acta Crystallogr A Found Adv* 2015;**71**:3-8.
3. Sheldrick GM. Crystal structure refinement with SHELXL. *Acta Crystallogr C Struct Chem* 2015;**71**:3-8.

Fractions A-E were all analysed by LC-MS and only the residual fraction E was the target one. Liquid chromatography was performed on an Agilent 6520B Q-TOF mass instrument. Chromatographic separation was achieved on an Agilent 1200 series with a DAD detector and a 1200 series bin pump equipped with a C_{18} column (4.6 × 150 mm, 5 μm, Shim-pack, Shimadzu) at 30 °C. The mobile phase consisted of A (H_2O) and B (MeOH). For the residual fraction, a gradient program was used according to the following profile: 0-10 min, 40-80% B, 10-20 min, 80-90% B, 20-30 min, 90-95% B, 30-40 min, 95% B. The flow rate was 1.0 mL/min, the injection volume was 5 μL for LC-MS analysis.

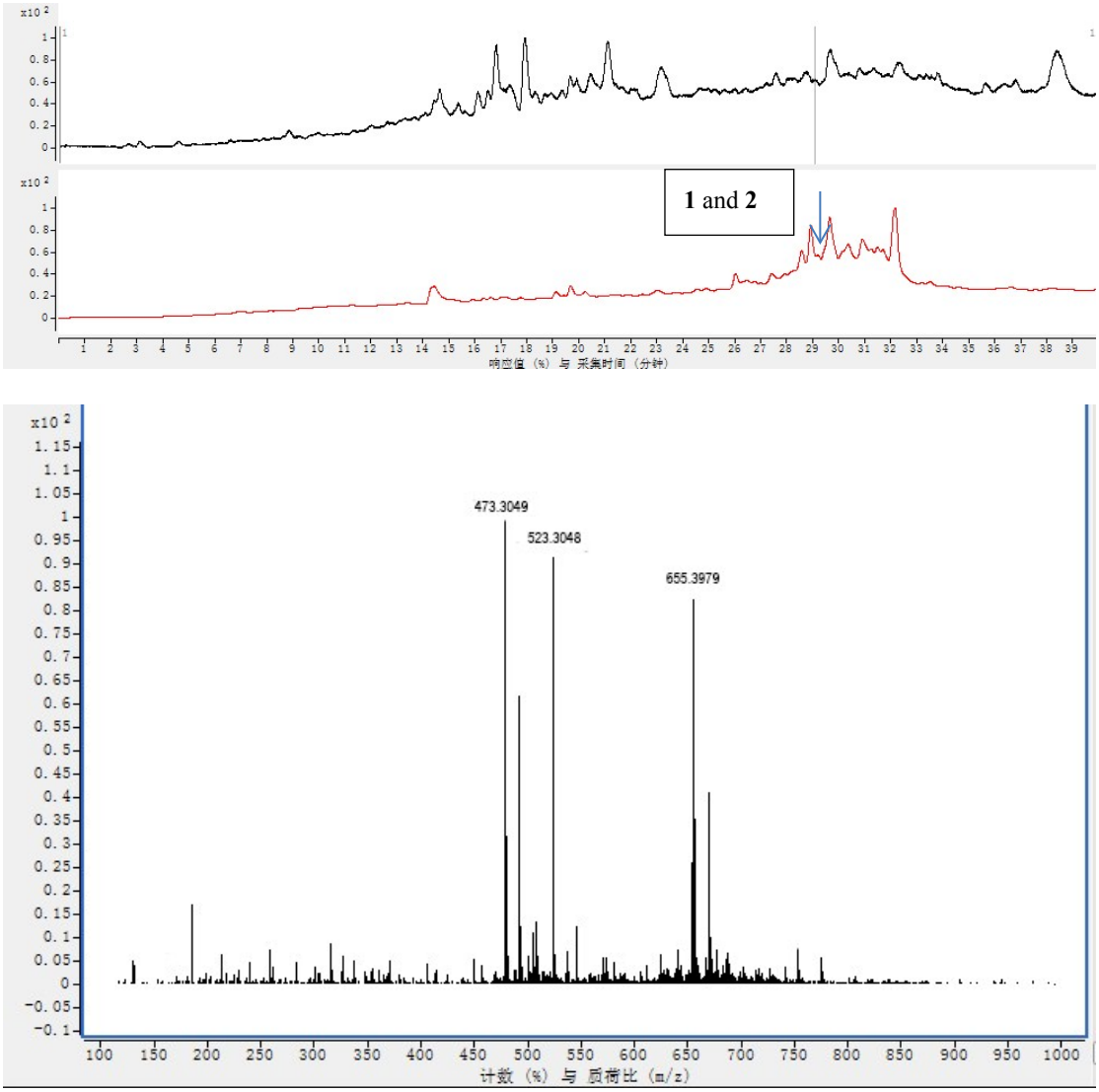

Figure S3 The HPLC-MS spectrum of the residual fraction E.

3. The computational details about compounds 1, 2, 1a, and 2a

3.1. Computational methods

All of the DFT calculations in this study were performed using the GAUSSIAN 09[1] packages. DFT method B3LYP with a standard 6-31G (d) basis set was used for the geometry optimizations and energy calculations. Frequency analyses were performed to assure that there were no imaginary frequencies.

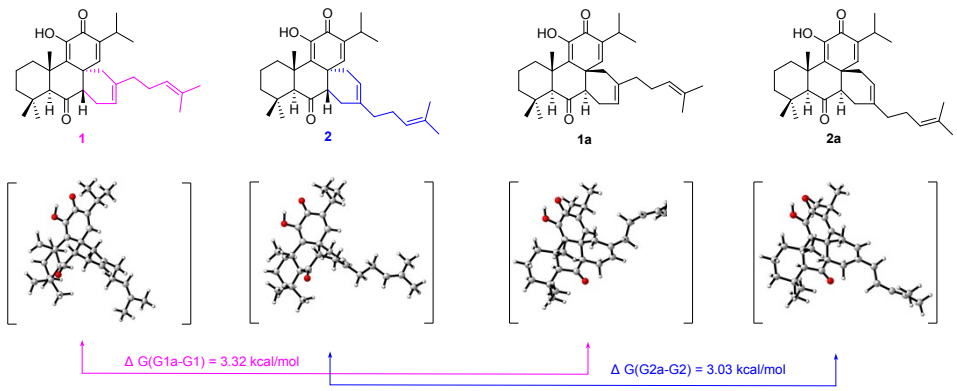

Figure S4 Comparison of energy for compounds **1**, **2**, **1a**, and **2a** at B3LYP/6-31G(d) level.

3.2. B3LYP geometries for all the optimized compounds

Compound 1

Energy: -874826.0376481

Number of Imaginary Frequencies: 0

O	4.56915	1.19986	1.58653
C	3.54806	1.02822	0.90326
C	3.07639	1.96011	-0.12796
C	3.85587	3.22838	-0.43885
C	3.90907	4.18619	0.76751
C	5.26918	2.92286	-0.97236
C	1.93301	1.64301	-0.76448
C	1.05873	0.44447	-0.49528
C	-0.24807	1.06766	0.14541
C	-1.25561	1.60710	-0.84679
C	-2.42059	2.37938	-0.26370
C	-3.42329	1.50358	0.53231
C	-4.54937	2.31575	1.11322
C	-5.85935	2.25883	0.82630

C	-6.48799	1.31472	-0.16980
C	-6.84015	3.17627	1.51841
C	-1.13731	1.41277	-2.16777
C	-0.03011	0.64600	-2.83788
C	0.75743	-0.25222	-1.86215
H	1.72628	-0.48443	-2.32506
C	0.06019	-1.62324	-1.73436
C	-0.23597	-2.10753	-0.32712
H	-0.90003	-1.33198	0.07439
C	-1.10356	-3.40775	-0.20193
C	-2.47522	-3.13786	-0.86538
C	-0.51705	-4.67869	-0.85731
C	-1.35455	-3.65025	1.30858
C	-0.08428	-3.64482	2.16425
C	0.69399	-2.33042	2.01608
C	1.07628	-2.00295	0.54352
C	2.17310	-2.97860	0.03260
C	1.67556	-0.57867	0.44493
C	2.79597	-0.23260	1.12536
O	3.41961	-1.03592	2.02788
O	-0.20606	-2.23801	-2.75224
H	3.30287	3.73708	-1.24117
H	4.40961	5.11983	0.48499
H	2.90127	4.43740	1.11828
H	4.46148	3.73791	1.59752
H	5.22723	2.27389	-1.85471
H	5.77133	3.85362	-1.26146

H	5.87571	2.42828	-0.20906
H	1.53719	2.34283	-1.49813
H	-0.73211	0.34482	0.80959
H	0.06829	1.87803	0.81642
H	-2.04390	3.17096	0.40192
H	-2.96555	2.88305	-1.07063
H	-3.79373	0.70956	-0.12463
H	-2.88880	1.00254	1.35282
H	-4.23340	3.05336	1.85401
H	-5.76683	0.66255	-0.66761
H	-7.23545	0.67595	0.32100
H	-7.02482	1.87602	-0.94716
H	-6.34411	3.84588	2.22808
H	-7.38529	3.79406	0.79080
H	-7.59980	2.60183	2.06719
H	-1.88497	1.85074	-2.82890
H	0.65314	1.34362	-3.34459
H	-0.43276	0.00499	-3.63017
H	-2.38527	-3.05025	-1.95047
H	-3.16405	-3.96243	-0.64469
H	-2.93187	-2.21623	-0.48082
H	0.32105	-5.10309	-0.29975
H	-1.29544	-5.45088	-0.89535
H	-0.19011	-4.48032	-1.87973
H	-2.02800	-2.86379	1.68293
H	-1.89478	-4.59891	1.42940
H	0.55576	-4.49747	1.90541

H	-0.35147	-3.78271	3.21993
H	1.59951	-2.34929	2.62689
H	0.07306	-1.50900	2.40275
H	1.89678	-4.02142	0.19138
H	2.35496	-2.84722	-1.04010
H	3.10983	-2.79998	0.56353
H	4.20344	-0.50497	2.30589

Compound 2

Energy: -874826.3666702

Number of Imaginary Frequencies: 0

O	-2.96252	4.02095	-0.20722
C	-2.18530	3.05761	-0.12412
C	-0.74373	3.17679	0.12586
C	-0.10316	4.54267	0.31705
C	-0.22432	5.42141	-0.94344
C	-0.65161	5.27013	1.56027
C	-0.03152	2.03469	0.16340
C	-0.55658	0.64117	-0.07125
C	0.10252	0.21737	-1.44685
C	1.48273	-0.36719	-1.31878
C	2.11827	-0.64927	-0.17283
C	3.51700	-1.22362	-0.16727
C	4.58283	-0.27953	0.44707
C	5.95009	-0.90831	0.46354
C	7.05865	-0.52556	-0.18919
C	7.15818	0.67712	-1.09602

C	8.34375	-1.30764	-0.04960
C	1.47310	-0.39650	1.17245
C	-0.06235	-0.27000	1.10011
H	-0.40425	0.19397	2.03552
C	-0.69821	-1.67663	1.11936
C	-1.70427	-1.98381	0.02566
H	-1.12129	-1.87480	-0.89748
C	-2.21798	-3.46308	-0.05620
C	-1.00083	-4.38251	-0.31612
C	-2.93891	-4.00059	1.20132
C	-3.15043	-3.56128	-1.29050
C	-4.25180	-2.49696	-1.33291
C	-3.67106	-1.07764	-1.28161
C	-2.77314	-0.82419	-0.03618
C	-3.63025	-0.77512	1.25917
C	-2.07164	0.55102	-0.14915
C	-2.78058	1.70287	-0.24049
O	-4.13400	1.75808	-0.35991
O	-0.37076	-2.45160	2.00110
H	0.96663	4.35679	0.48859
H	-1.27086	5.65233	-1.15862
H	0.31396	6.36523	-0.79695
H	0.20620	4.92025	-1.81822
H	-0.52677	4.66032	2.46253
H	-0.11284	6.21269	1.71309
H	-1.71433	5.49754	1.44213
H	1.04690	2.10025	0.29585

H	0.13545	1.10674	-2.09037
H	-0.54435	-0.48161	-1.98938
H	1.98582	-0.57581	-2.26351
H	3.51997	-2.16640	0.40046
H	3.81905	-1.47284	-1.19135
H	4.57852	0.66571	-0.10619
H	4.29048	-0.03627	1.47913
H	6.02174	-1.80444	1.08354
H	7.92046	1.37802	-0.72793
H	7.47755	0.37573	-2.10343
H	6.21922	1.22676	-1.19438
H	8.22779	-2.17012	0.61422
H	8.69249	-1.67360	-1.02574
H	9.15017	-0.67680	0.35045
H	1.90136	0.50515	1.63200
H	1.70373	-1.21613	1.86295
H	-0.34555	-4.43525	0.55617
H	-1.34439	-5.39814	-0.54752
H	-0.40871	-4.03245	-1.17179
H	-3.93993	-3.58450	1.33665
H	-3.05824	-5.08700	1.10540
H	-2.35663	-3.80545	2.10395
H	-2.53858	-3.46307	-2.20063
H	-3.58838	-4.56803	-1.32356
H	-4.96222	-2.64693	-0.51019
H	-4.83596	-2.60945	-2.25533
H	-4.47116	-0.33430	-1.30705

H	-3.06292	-0.91431	-2.18354
H	-4.27305	-1.65035	1.35549
H	-2.99816	-0.73335	2.15340
H	-4.27151	0.10806	1.25093
H	-4.32571	2.72590	-0.36747

Compound 1a

Energy: -874823.0096451

Number of Imaginary Frequencies: 0

O	-0.04997	4.09470	-1.00044
C	0.03036	2.98069	-0.46044
C	-0.80510	2.54837	0.66047
C	-1.80918	3.49853	1.29381
C	-1.12800	4.73792	1.90595
C	-2.92462	3.90186	0.30926
C	-0.65907	1.27359	1.06622
C	0.26033	0.24315	0.46226
C	-0.68593	-0.71014	-0.36728
C	-1.63128	-1.54789	0.46736
C	-2.86217	-2.07598	-0.23575
C	-3.98131	-1.01574	-0.40781
C	-5.13615	-1.53335	-1.22242
C	-6.40069	-1.76331	-0.83561
C	-6.93864	-1.51923	0.55341
C	-7.41884	-2.30469	-1.81180
C	-1.36137	-1.83305	1.74555
C	-0.15824	-1.33442	2.49708

C	0.88341	-0.59805	1.63610
H	1.43757	0.10426	2.27228
C	1.91501	-1.54319	1.02319
C	3.07845	-0.80951	0.38099
H	3.30974	0.01018	1.07882
C	4.41614	-1.61460	0.27670
C	4.81813	-2.06480	1.69985
C	4.37082	-2.87534	-0.61524
C	5.49345	-0.63029	-0.23499
C	5.08278	0.09881	-1.51496
C	3.75512	0.85746	-1.36712
C	2.56101	-0.03424	-0.90587
C	2.15828	-0.96935	-2.08297
C	1.33421	0.82469	-0.47286
C	1.08126	2.05963	-0.98296
O	1.77585	2.65031	-1.98638
O	1.76951	-2.75342	1.03734
H	-2.28028	2.94063	2.11549
H	-0.65213	5.34442	1.13084
H	-1.86990	5.35893	2.42145
H	-0.36377	4.44946	2.63698
H	-3.43852	3.01909	-0.08855
H	-3.66959	4.52403	0.81927
H	-2.51752	4.47193	-0.52992
H	-1.31279	0.90303	1.85112
H	-0.08037	-1.38987	-0.97356
H	-1.24041	-0.08754	-1.07925

H	-2.58418	-2.45828	-1.22947
H	-3.27071	-2.92749	0.32077
H	-4.30128	-0.68240	0.58469
H	-3.56042	-0.13047	-0.90779
H	-4.88366	-1.76373	-2.25970
H	-6.18710	-1.13986	1.24959
H	-7.76724	-0.79766	0.52770
H	-7.35004	-2.44652	0.97605
H	-7.83387	-3.26050	-1.46160
H	-8.27051	-1.61784	-1.91799
H	-6.98776	-2.46584	-2.80494
H	-2.04699	-2.46845	2.30603
H	0.34122	-2.18530	2.97654
H	-0.48503	-0.67935	3.31874
H	4.13265	-2.82051	2.09394
H	5.82445	-2.50047	1.68420
H	4.83880	-1.21755	2.39779
H	4.24150	-2.64619	-1.67511
H	5.32038	-3.41608	-0.51598
H	3.56347	-3.54214	-0.30752
H	5.69036	0.11635	0.54950
H	6.43571	-1.17382	-0.38745
H	5.86002	0.82163	-1.79432
H	5.02820	-0.61056	-2.35052
H	3.51030	1.33734	-2.31428
H	3.88939	1.66661	-0.63711
H	1.46544	-0.44867	-2.75122

H	3.02927	-1.25122	-2.67853
H	1.68839	-1.89807	-1.74879
H	1.35524	3.54072	-2.06316

Compound 2a

Energy: -874823.0446539

Number of Imaginary Frequencies: 0

O	4.17648	2.92136	-0.56855
C	3.12622	2.30750	-0.32501
C	1.95051	2.90898	0.30430
C	1.97147	4.35635	0.77008
C	3.03195	4.59926	1.86135
C	2.14288	5.34013	-0.40424
C	0.85764	2.13105	0.40975
C	0.72091	0.71108	-0.07577
C	-0.17370	0.81587	-1.37284
C	-1.61093	1.17196	-1.09863
C	-2.23397	0.99072	0.07109
C	-3.70109	1.30709	0.25430
C	-4.60644	0.04701	0.26559
C	-6.04476	0.38531	0.55087
C	-7.11665	0.23576	-0.24307
C	-7.08595	-0.34089	-1.63775
C	-8.49090	0.64809	0.23046
C	-1.49753	0.45966	1.27911
C	-0.08898	-0.09328	1.00590
H	0.49299	-0.04701	1.93582

C	-0.10813	-1.55812	0.57557
C	1.27510	-2.18165	0.54816
H	1.76811	-1.80123	1.45606
C	1.32224	-3.73748	0.70925
C	0.64237	-4.54831	-0.41615
C	0.62260	-4.10545	2.03772
C	2.81295	-4.13150	0.83134
C	3.67532	-3.57950	-0.30436
C	3.58195	-2.05159	-0.43101
C	2.12828	-1.51654	-0.61601
C	1.64161	-1.89667	-2.04494
C	2.05357	0.02982	-0.42741
C	3.10477	0.85668	-0.67368
O	4.29209	0.47810	-1.20733
O	-1.14275	-2.12565	0.26892
H	0.98589	4.54547	1.21847
H	2.96448	5.63004	2.22856
H	2.88391	3.92717	2.71460
H	4.03978	4.44078	1.46837
H	1.35965	5.19694	-1.15761
H	2.07749	6.37304	-0.04229
H	3.11459	5.20625	-0.88680
H	-0.05372	2.57126	0.80557
H	0.28806	1.55442	-2.03901
H	-0.14635	-0.13242	-1.91707
H	-2.17251	1.56297	-1.94727
H	-3.84885	1.85404	1.19808

H	-4.04083	1.97301	-0.54786
H	-4.49063	-0.47413	-0.68945
H	-4.24132	-0.64826	1.03478
H	-6.21507	0.82169	1.53779
H	-7.72083	-1.23581	-1.70134
H	-7.49324	0.37824	-2.36225
H	-6.08333	-0.61934	-1.96978
H	-8.92792	1.40728	-0.43382
H	-9.18489	-0.20451	0.22439
H	-8.46819	1.05815	1.24519
H	-1.44059	1.25493	2.03779
H	-2.08590	-0.34253	1.74005
H	0.64646	-5.61086	-0.14199
H	-0.39421	-4.23484	-0.55203
H	1.15520	-4.46317	-1.37664
H	1.03993	-3.53918	2.88071
H	-0.45386	-3.91694	1.99437
H	0.76775	-5.17069	2.25439
H	2.89401	-5.22590	0.87915
H	3.20164	-3.75052	1.78811
H	4.72656	-3.84491	-0.13375
H	3.40128	-4.06122	-1.25143
H	4.01129	-1.59513	0.47049
H	4.20133	-1.72271	-1.26504
H	2.07696	-2.84399	-2.37041
H	0.55598	-2.00622	-2.11185
H	1.95990	-1.13416	-2.76258

H 4.82243 1.31142 -1.20064

1. Gaussian 09, Revision D.01, M. J. Frisch, G. W. Trucks, H. B. Schlegel, G. E. Scuseria, M. A. Robb, J. R. Cheeseman, G. Scalmani, V. Barone, B. Mennucci, G. A. Petersson, H. Nakatsuji, M. Caricato, X. Li, H. P. Hratchian, A. F. Izmaylov, J. Bloino, G. Zheng, J. L. Sonnenberg, M. Hada, M. Ehara, K. Toyota, R. Fukuda, J. Hasegawa, M. Ishida, T. Nakajima, Y. Honda, O. Kitao, H. Nakai, T. Vreven, J. A. Montgomery, Jr., J. E. Peralta, F. Ogliaro, M. Bearpark, J. J. Heyd, E. Brothers, K. N. Kudin, V. N. Staroverov, T. Keith, R. Kobayashi, J. Normand, K. Raghavachari, A. Rendell, J. C. Burant, S. S. Iyengar, J. Tomasi, M. Cossi, N. Rega, J. M. Millam, M. Klene, J. E. Knox, J. B. Cross, V. Bakken, C. Adamo, J. Jaramillo, R. Gomperts, R. E. Stratmann, O. Yazyev, A. J. Austin, R. Cammi, C. Pomelli, J. W. Ochterski, R. L. Martin, K. Morokuma, V. G. Zakrzewski, G. A. Voth, P. Salvador, J. J. Dannenberg, S. Dapprich, A. D. Daniels, O. Farkas, J. B. Foresman, J. V. Ortiz, J. Cioslowski, and D. J. Fox, Gaussian, Inc., Wallingford CT, 2013.

4. The details of biomimetic synthesis of compounds 1 and 2

4.1. Reagents and solvents

All used chemical reagents were supplied by Sigma-Aldrich, Aladdin, and Macklin. MeOH, ACN, CH_2Cl_2, and toluene were anhydrous solvents.

4.2. General procedure for the biomimetic synthesis of compounds 1 and 2.

Most of entries were added taxodione (**3**) (10.0 mg, 0.032 mmol, 1 equiv) and myrcene (**4**) (21.8 mg, 0.16 mmol, 5 equiv) in CH_2Cl_2 (1.0 mL). Stirring the mixture in

EtOH at RT or at reflux for 10 d (entries 1 and 2), the DA reaction did not occur. In view of compound **3** being dissolved in **4** (entry 3), the mixture of **3** and **4** was stirred for 10 d at room temperature, while there were no products observed. All the above results showed that compounds **1** and **2** were not the artifacts produced during the separation progress. Subsequently, the thermal cycloaddition was considered : (1) We added **3** (9.9 mg, 0.032 mmol, 1 equiv) and **4** (21.9 mg, 0.16 mmol, 5 equiv) in CH_2Cl_2 (1 ml) and added $BF_3{\cdot}OEt_2$ (20 μl, 0.016 mmol, 0.5 equiv) into it. The mixture was stirred at 40 ℃ under nitrogen for 24 h (entry 4). (2) Then the DA reaction was performed according to Deng's research[1] ($Er(fod)_3$, neat, 120°C) (entry 5). (3) The mixture of **3** and **4** with $Er(fod)_3$ in CH_2Cl_2 was stirred at 100 °C for 1 d (entry 6). In fact, this protocol was designed to keep high reaction temperature according to previous research works, in which the reaction was performed in a sealed tube over 100 ℃ with low boiling solvents (such as CH_2Cl_2 or $CHCl_3$).[2] (4) To a stirred mixture solution of **3** (10.0 mg, 0.032 mmol, 1 equiv) and **4** (21.8 mg, 0.16 mmol, 5 equiv) in toluene (1 ml) was added $Er(fod)_3$ (16.8mg, 0.016 mmol, 0.5 equiv) was stirred at 80 ℃ for 1 h firstly. Then the mixture was warmed to 100 ℃ for 1 h. At last the mixture was warmed at 120 ℃ for 24 h (entry 7). There were no products being detected under all the mentioned thermal cycloaddition conditions. Then we considered the photocycloadditions combining with catalyst $Er(fod)_3$ for the DA reaction. Firstly, the mixture of **3** and **4** was added the catalyst $Er(fod)_3$ in it (solvent-free) and was stirred under 365 nm at rt for 10 d (entry 8) but the DA reaction did not occur. The mixture of **3** and **4** with $Er(fod)_3$ was added in CH_2Cl_2 and was stirred under UV (365 nm) irradiating at room

temperature for two days, and a trace of compounds **1** and **2** were detected (Figure S4d). After 10 days, compound **3** transformed completely and we obtained compounds **1** (4.35 mg) and **2** (4.55 mg) (Figure S4e) using NP-HPLC CC (*n*-hexane:isopropanol = 98:2, 1.0 mL/min). Increasing the reaction temperature (60 °C) or increasing the equivalent of catalyst (300%) (entries 9 and 10), the reaction speed was constant. Temperature and the equivalent of catalyst are not the key factor in this DA reaction. Changing the lighting conditions (entries 11 and 12), the DA reaction did not occur. The result showed that UV (365 nm) was necessary for this DA reaction. To screen the excellent catalyst, we replaced KI, $CuSO_4$, $AlCl_3$ and $ZnCl_2$ with $Er(fod)_3$ (entries 13-16) and the result showed that $Er(fod)_3$ was the best choice.

The UV light was generated using an ultraviolet analyzer. The photocycloaddition was done in the penicillin bottle without plug under the UV light condition. The environment of this reaction was open so that it can keep at room temperature.

Table S2 Conditions screen for the biomimetic synthesis of compounds **1** and **2**.

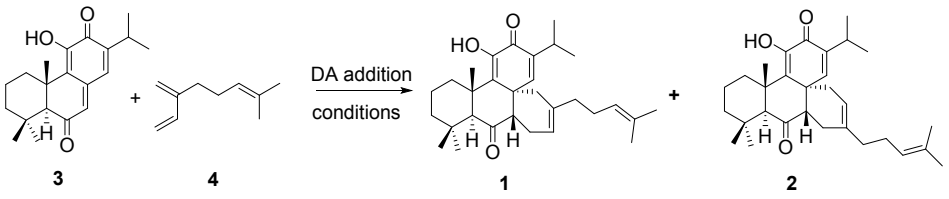

Entry[a]	solvent	*t* (°C)	light	catalyst	mol%	time	Conversion[b] (%)
1	EtOH	RT	-[f]	-	-	10 d	0
2	EtOH	reflux	-[f]	-	-	10 d	0
3	-[c]	RT	-[f]	-	-	10 d	0

4	CH_2Cl_2	40	-[f]	$BF_3{\cdot}OEt_2$	50	1 d	0
5	-[e]	120	-[f]	$Er(fod)_3$	50	1 d	0
6	CH_2Cl_2	100	-[f]	$Er(fod)_3$	50	1 d	0
7	toluene	-[d]	-[f]	$Er(fod)_3$	50	1 d	0
8	-[c]	RT	UV (365)	$Er(fod)_3$	50	10 d	0
9	CH_2Cl_2	60	UV (365)	$Er(fod)_3$	50	10 d	100
10	CH_2Cl_2	RT	UV (365)	$Er(fod)_3$	300	10 d	100
11	CH_2Cl_2	RT	-[f]	$Er(fod)_3$	50	10 d	0
12	CH_2Cl_2	RT	UV (254)	$Er(fod)_3$	50	10 d	0
13	CH_2Cl_2	RT	UV (365)	KI	50	10 d	trace
14	CH_2Cl_2	RT	UV (365)	$CuSO_4$	50	10 d	0
15	CH_2Cl_2	RT	UV (365)	$AlCl_3$	50	10 d	0
16	CH_2Cl_2	RT	UV (365)	$ZnCl_2$	50	10 d	trace

[a] the formation of side products in DA reaction was not detected. [b] Conversions and the ratio of **1** and **2** (about 1:1) were determined by NP-HPLC. [c]Solvent-free and added **4** (218.0 mg, 1.6 mmol) and **3** (10.0 mg, 0.032 mmol, compound **3** can dissolve in compound **4**). [d]Temperature programming. [e]The condition was based on the reference. [f] No light source used. Thick-walled sealed tubes (15 ml) were used for entries 6, 7 and 9.

1 J. Deng, S. Zhou, W. Zhang, J. Li, R. Li and A. Li, *J. Am. Chem. Soc.*, 2014, **136**, 8185-8188.

2 (a) T. Matsubara, K. Takahashi, J. Ishihara and S. Hatakeyama, *Angew. Chem., Int. Ed. Engl.*, 2014, **53**, 757-760; (b) J. Duenas, A. Garcia-Granados, A. Martinez, E. Onorato and A. Parra, *J. Org. Chem.*, 1995, **60**, 2170-2173; (c) R. C. Conyers, C. L. Barnes and B. W. Gung, *Tetrahedron Lett.*, 2015, **56**, 3318-3321.

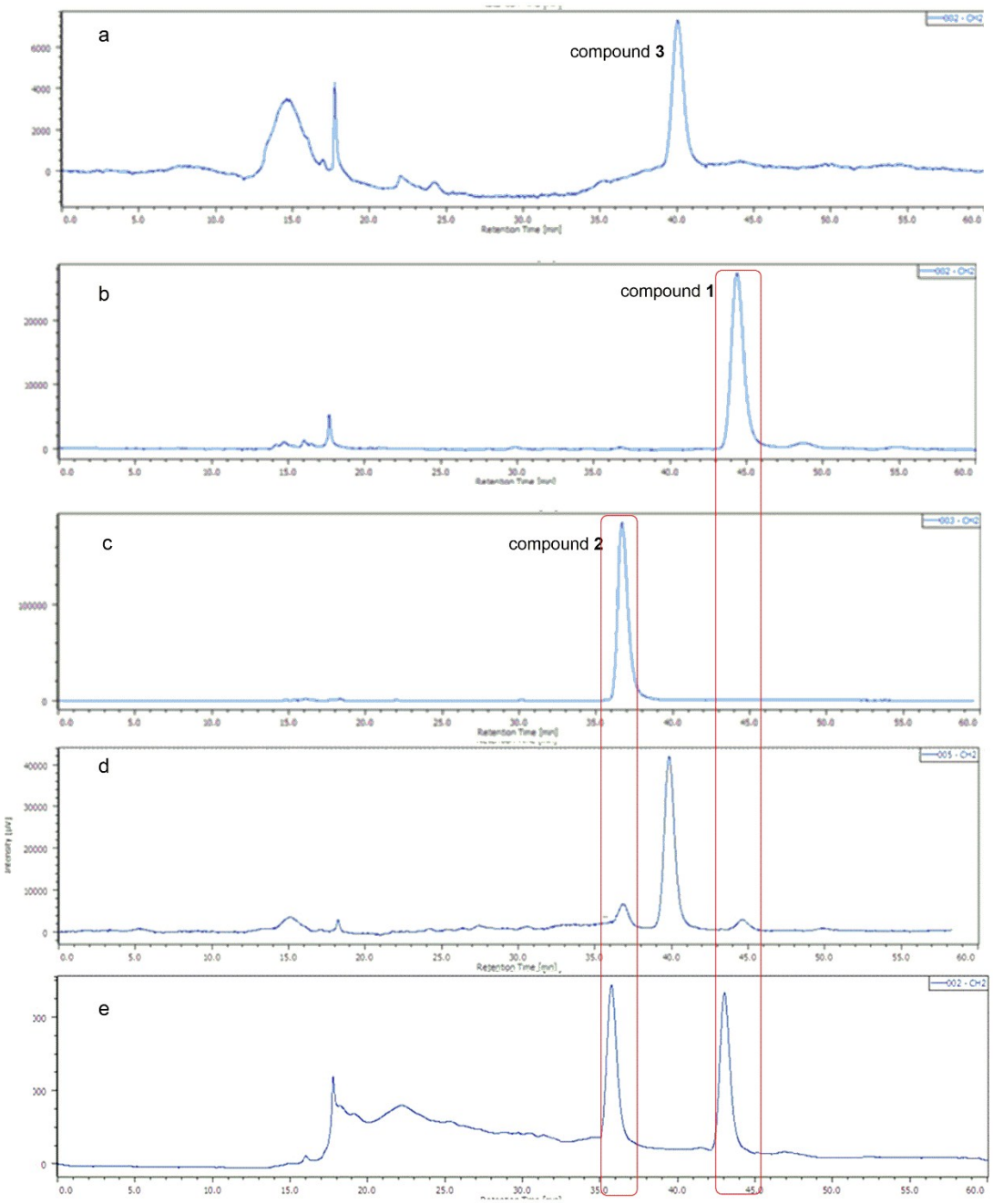

Figure S5 The natural and biomimetic synthesis of compounds **1** and **2** (NR-HPLC: *n*-hexane:isopropanol = 98:2, 1.0 mL/min) were detected using NP-HPLC. (a) Compound **3** was detected using NR-HPLC. (b) Compound **1** was detected using NP-HPLC. (c) Compound **2** was detected using NR-HPLC. (d) The mixture was detected using NR-HPLC after 2 days being stirred under UV (365 nm) light and $Er(fod)_3$ at room temperature and the result showed that **1** and **2** were observed in trace. (e) The mixture was detected using NP-HPLC and the result showed that compound **3** transformed completely for 10 days.

5. The details of inhibiting lipid accumulation assay

5.1 Cell culture and treatment

Human L02 cells were seeded into 96-well microplates and cultured in DMEM medium (Hyclone, USA) including 10% fetal bovine serum (Gemini, USA) and 1% penicillin/streptomycin (P/S) (Invitrogen, USA) at 37 °C with 5% CO_2 for 24 h. Then cells were treated with compounds **1** (20 μM) and **2** (5, 10, 20 μM) for 48 h, respectively, the 0.25 mM of FFA [palmitic acid-oil acid (1:2) was dissolved in medium] was added at the same time except the control group.[1] The parallel experimental groups were seeded into 24-well microplates and others were same with the aforementioned information.

5.2. Oil red O staining

The samples were measured according to the specification of oil red O stain kit (Cat#G1262, Solarbio, Beijing, China). And the parallel experimental groups were stained by oil red O (dissolved by the 60% EtOH) for 25 min, then eluted by the isopropanol and the absorbance was read at 490 nm with a Universal microplate reader (Spectramax Plus 384, Molecular Devices, Sunnyvale, CA, USA).

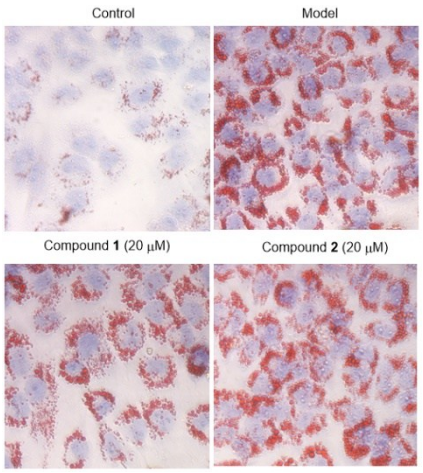

Figure S6 Compounds **1** and **2** inhibited the lipid accumulation in L02 cells treated with FFA at a concentration of 20 μM.

(A)

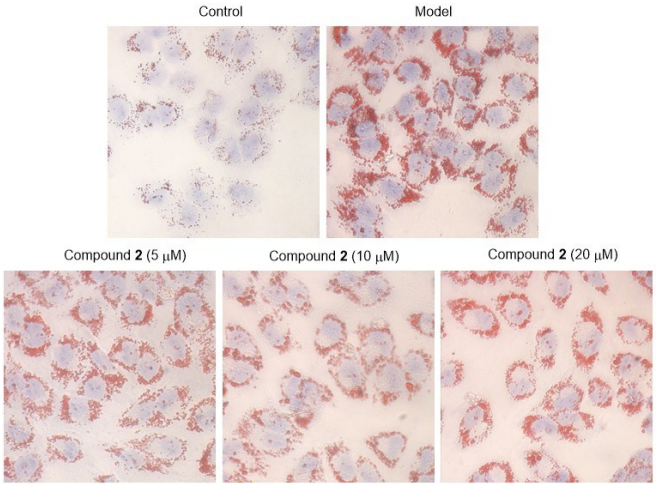

(B)

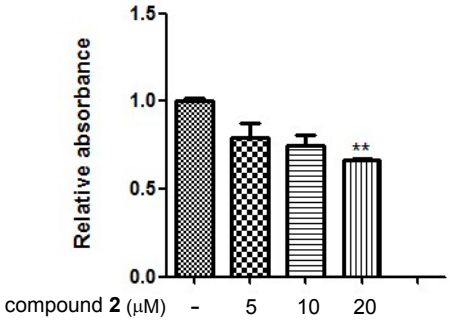

Figure S7 (A) Compound **2** inhibited the lipid accumulation in L02 cells treated with FFA. Control cells were treated with 100 μL blank medium. Model cells were treated with 0.25 mM FFA for 48 h. Other cells were treated with 0.25 mM FFA and **2** with different concentrations for 48 h. Cells were stained with Oil Red O kit and observed by optical microscopy (n = 3). (B) FFA-exposed L02 cells were treated with compound **2** for 48 h, dyed by oil red O, eluted with isopropanol, and measured the relative absorbance (n = 3, $^{**}P < 0.01$, compared with model).

1. Zhu X, Bian H, Wang L, Sun X, Xu X, Yan H, et al. Berberine attenuates nonalcoholic hepatic steatosis through the AMPK-SREBP-1c-SCD1 pathway. *Free Radic Biol Med* 2019;**141**: 192-204.

Table S3. The cytotoxicity of compounds **1**and **2** against L02 cells

Compounds	IC_{50} (μM)
1	>50
2	>50

All values are mean ± SD (n = 3)

6. The spectra of compounds 1 and 2.

TCM-CPU HR-ESI-MS Display Report

Sample Name: TDB-38-2 **Instrument:** Agilent 6520B Q-TOF

Acq. Date: 03/22/2019 **Operator:** Administrator

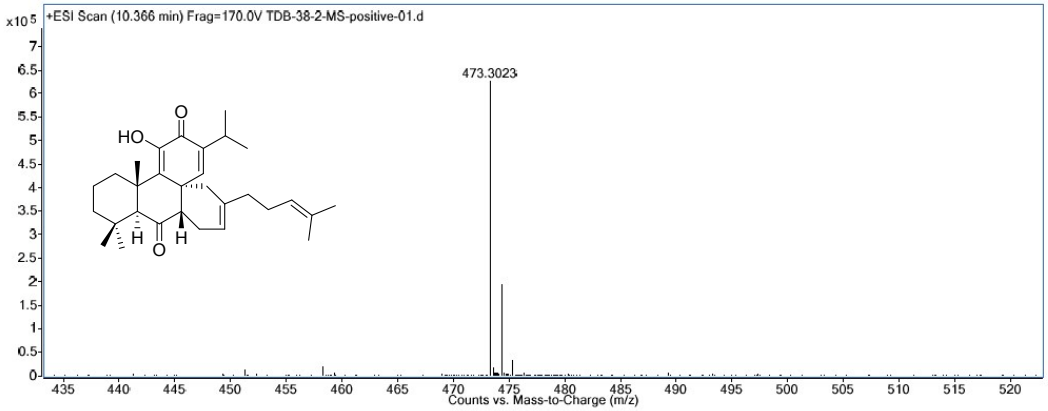

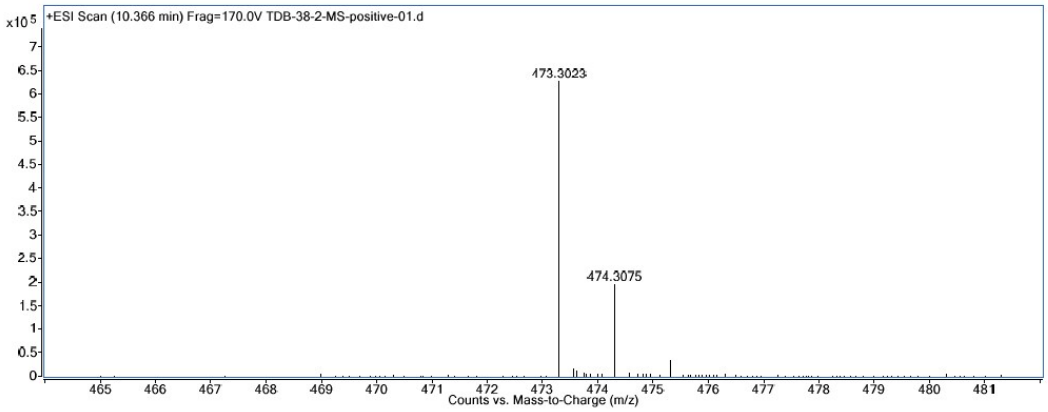

Elemental Composition Calculator

Target m/z:	473.3023	**Result type:**	Positive ions	**Species:**	$[M+Na]^+$
Elements:		C (0-80); H (0-120); O (0-30); Na (0-5)			
Ion Formula		**Calculated m/z**		**PPM Error**	
C30H42NaO3		473.3026		0.7	

Agilent Technologies

Figure S8 HRESIMS spectrum of compound **1** in MeOH.

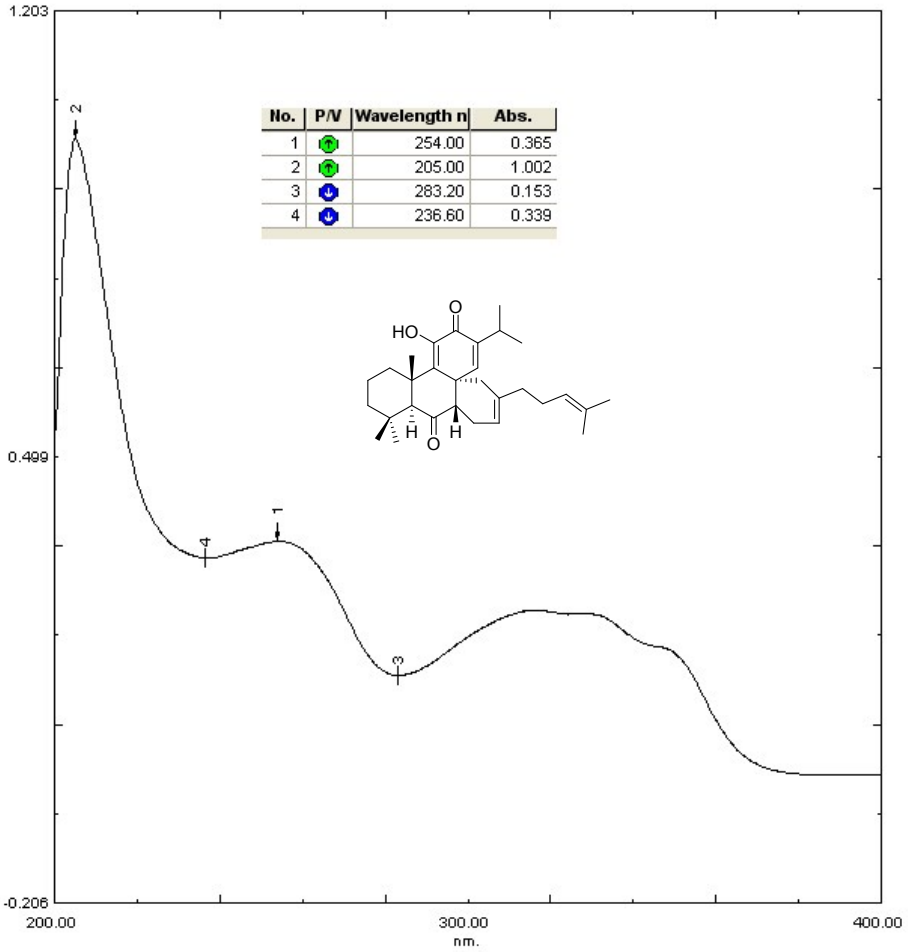

Figure S9 UV spectrum of compound **1** in MeOH.

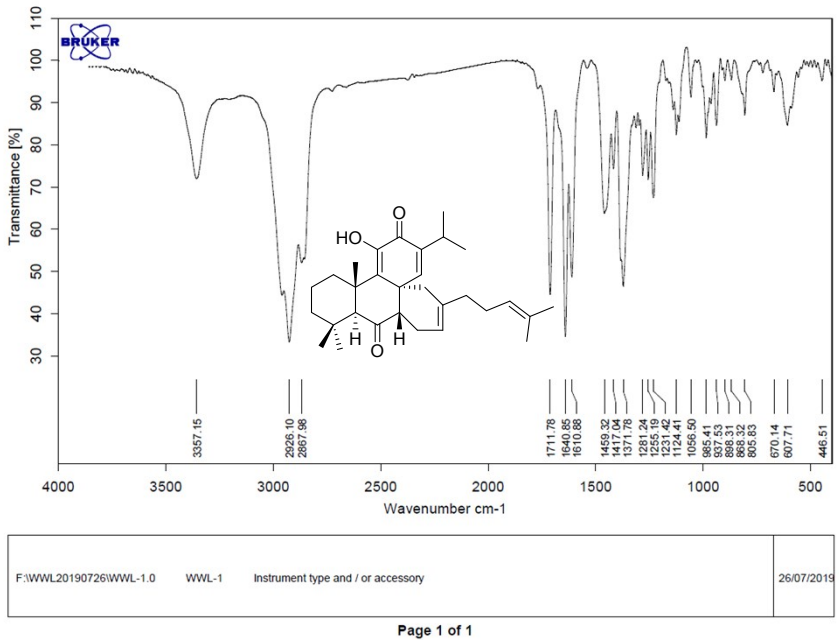

Figure S10 IR (KBr disc) spectrum of compound **1**.

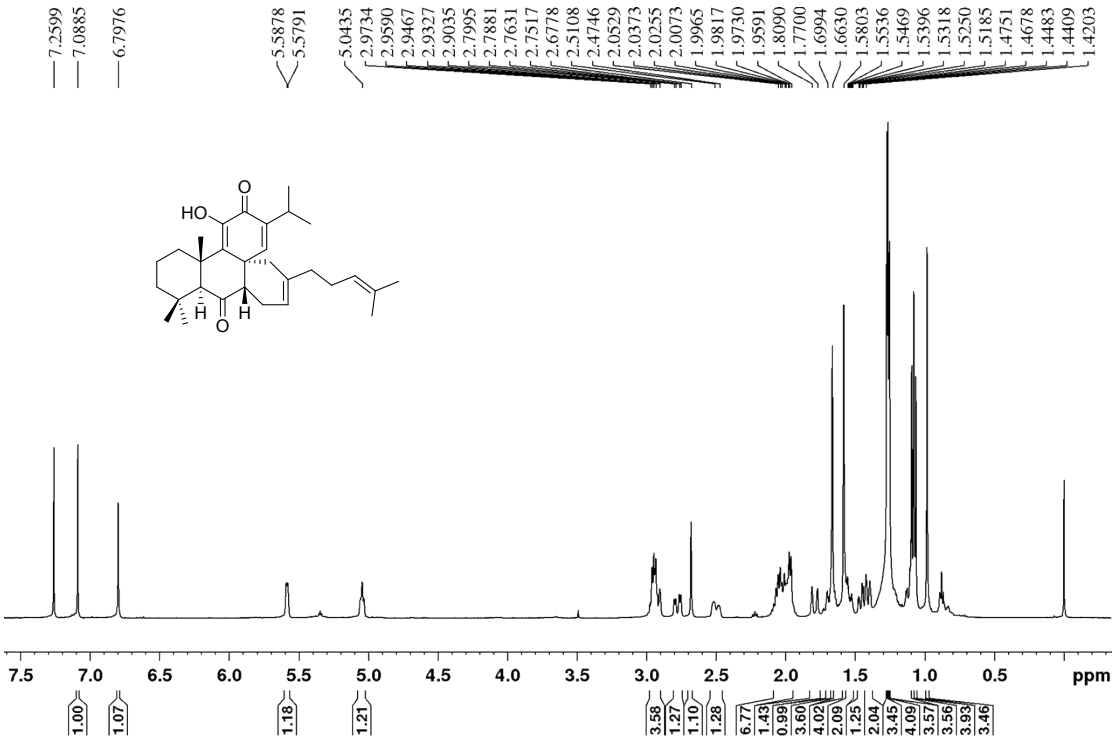

Figure S11 ^{1}H NMR spectrum of compound **1** in $CDCl_3$ (500 MHz).

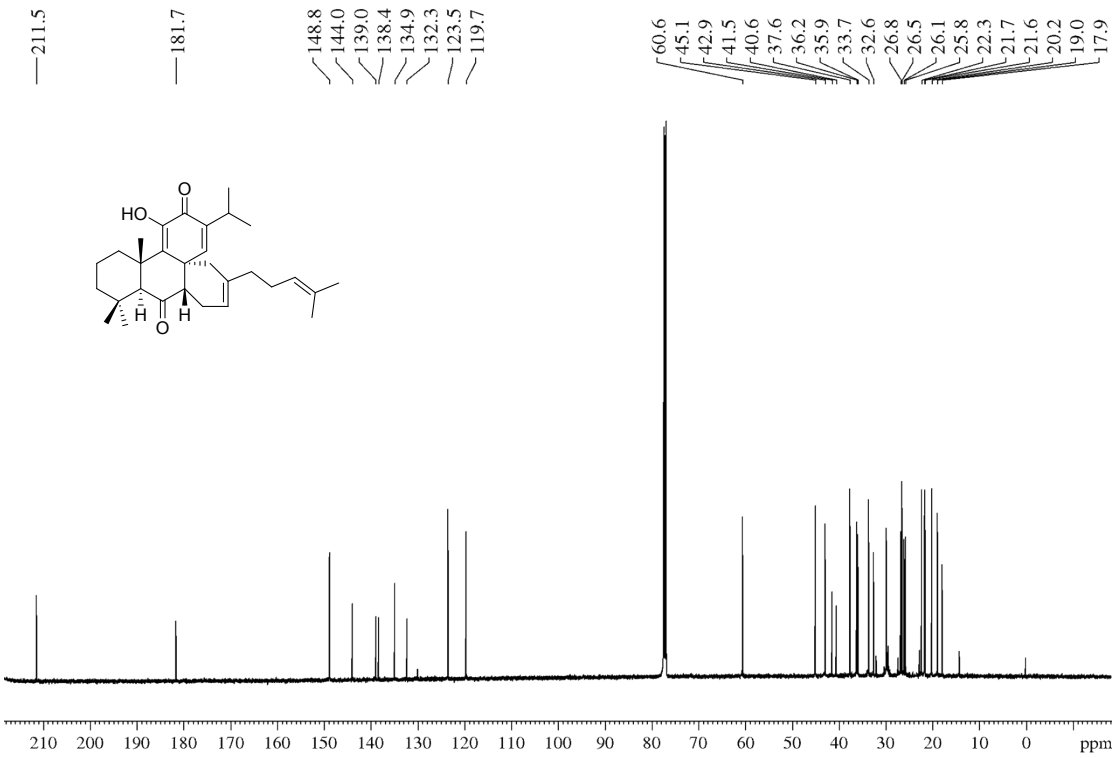

Figure S12 ^{13}C NMR spectrum of compound **1** in $CDCl_3$ (125 MHz).

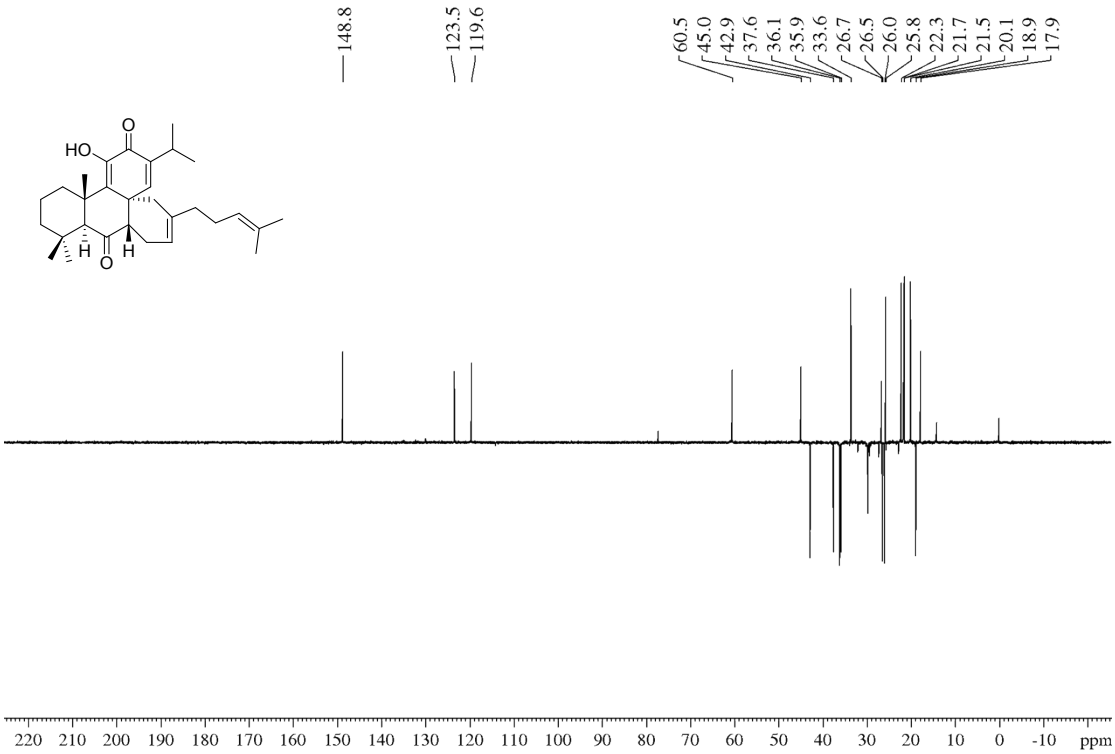

Figure S13 DEPT spectrum of compound **1** in $CDCl_3$ (150 MHz).

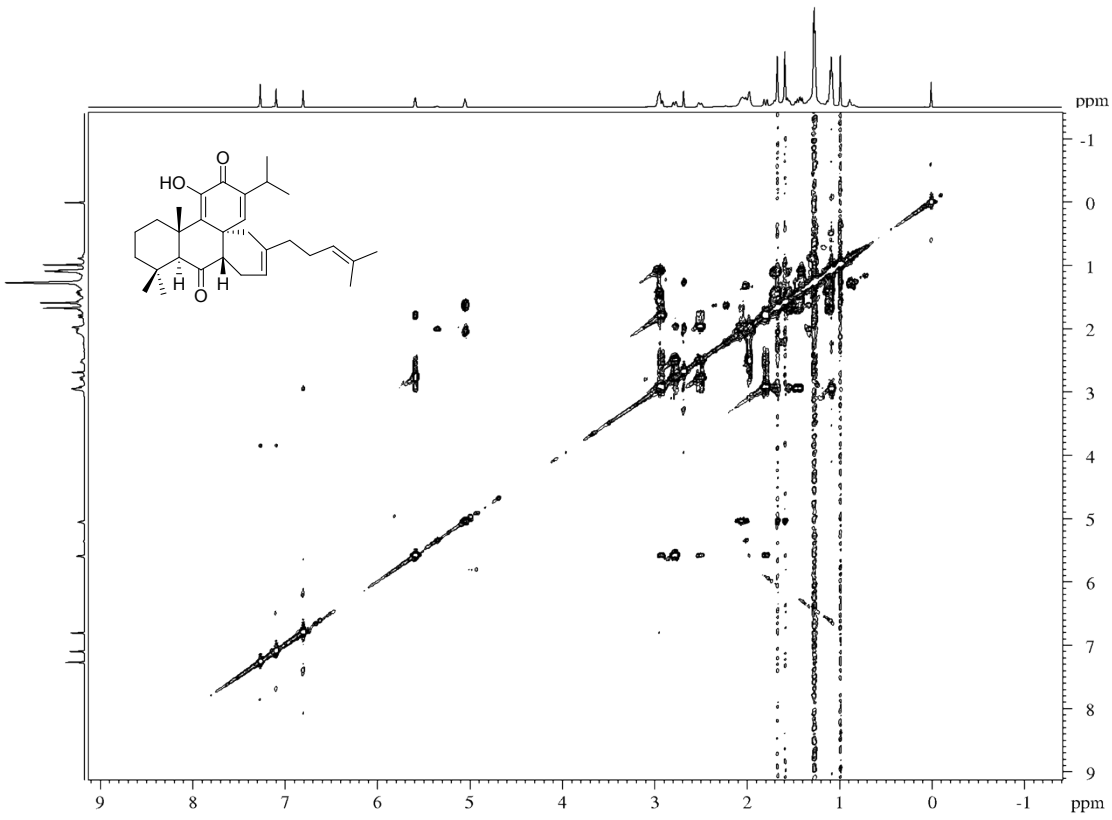

Figure S14 ^{1}H-^{1}H COSY spectrum of compound **1** in $CDCl_3$ (600 MHz).

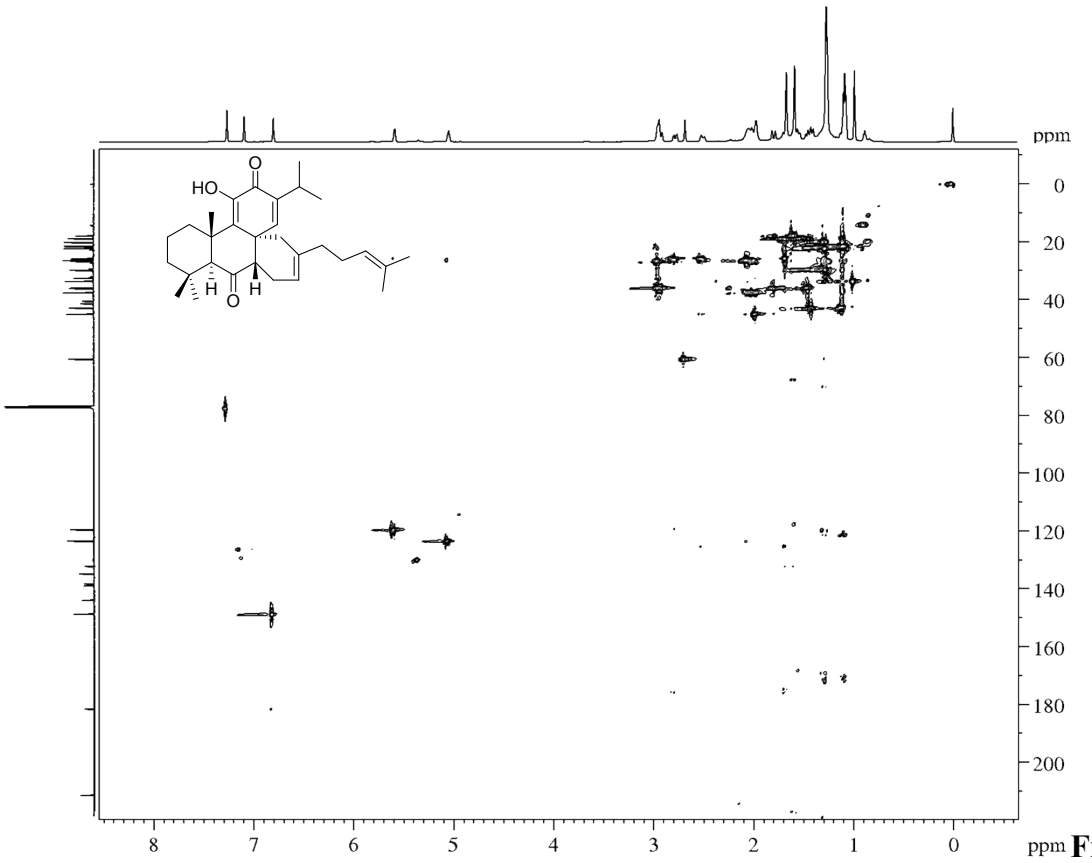

Figure S15 HSQC spectrum of compound **1** in $CDCl_3$ (600 MHz).

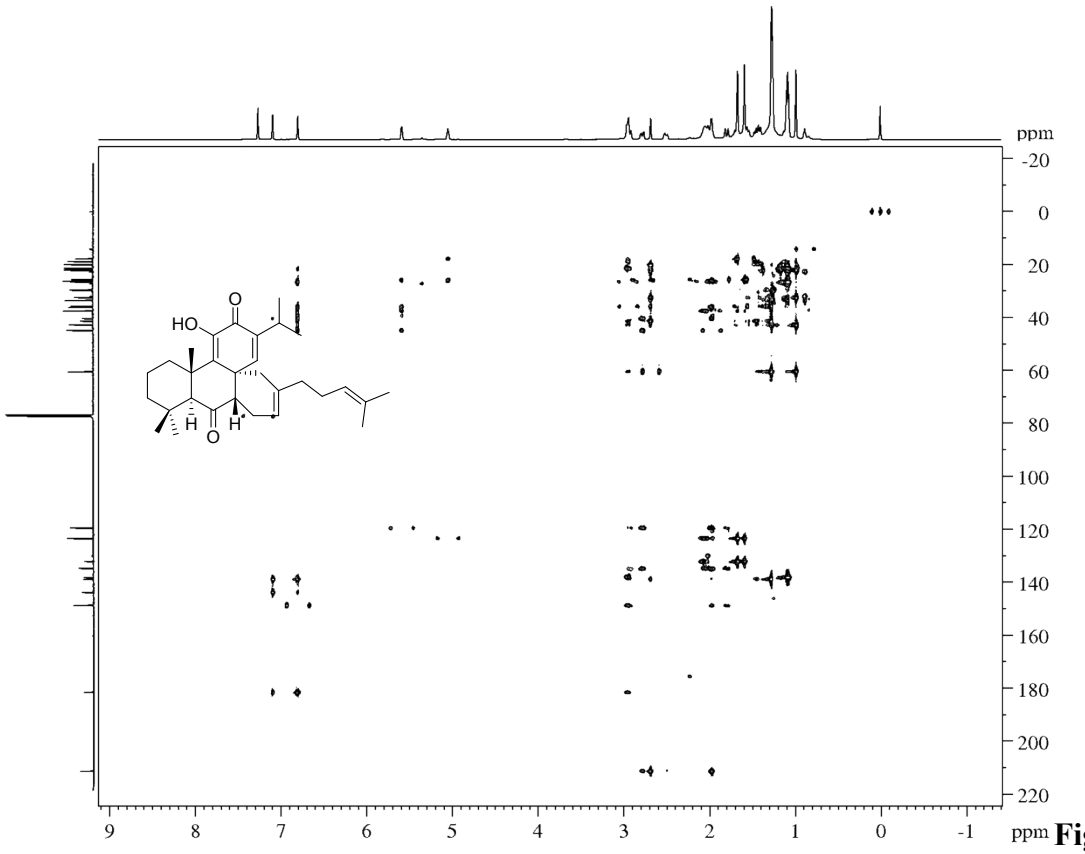

Figure S16 HMBC spectrum of compound **1** in $CDCl_3$ (600 MHz).

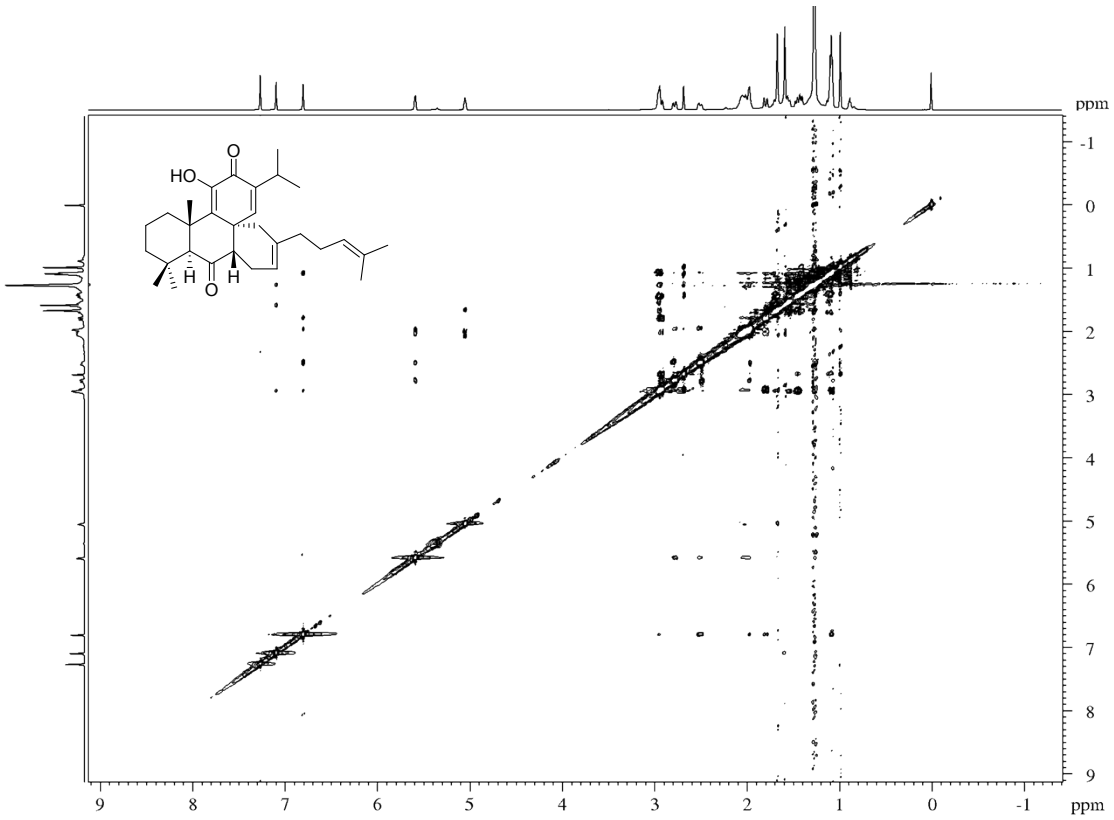

Figure S17 ROESY spectrum of compound **1** in $CDCl_3$ (600 MHz).

TCM-CPU HR-ESI-MS Display Report

Sample Name: TDB-38-1 **Instrument:** Agilent 6520B Q-TOF

Acq. Date: 03/22/2019 **Operator:** Administrator

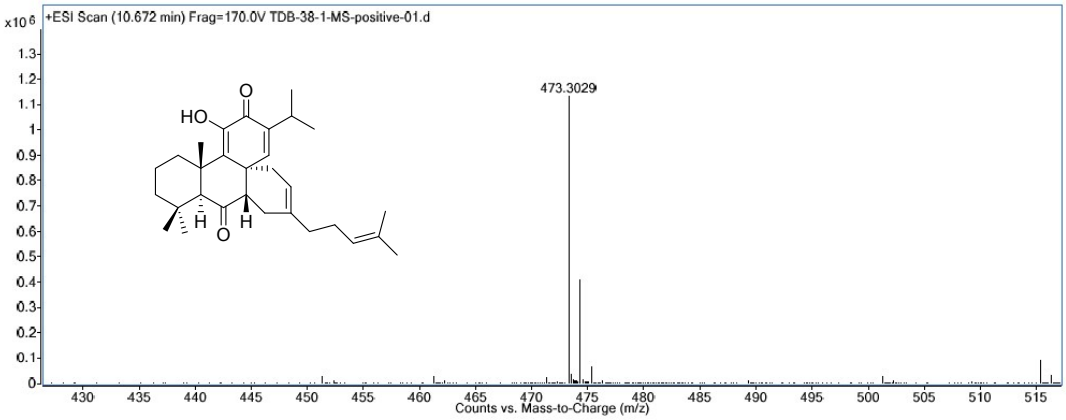

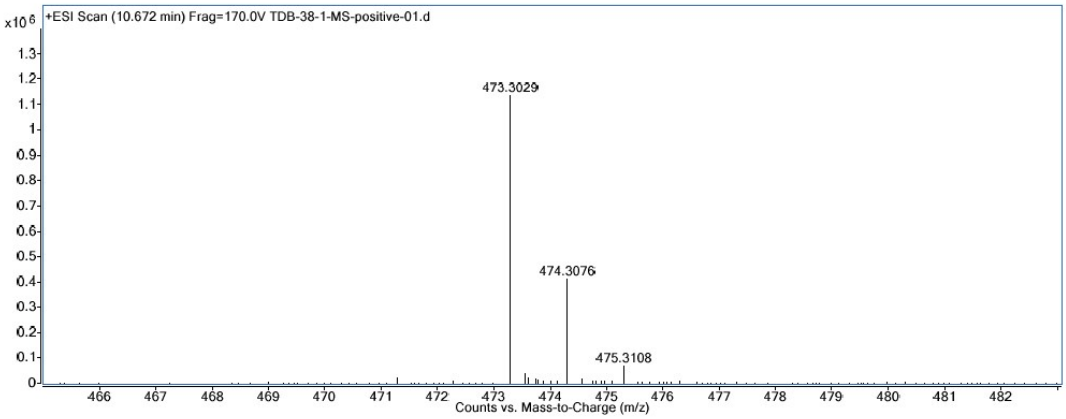

Elemental Composition Calculator

Target m/z:	473.3029	**Result type:**	Positive ions	**Species:**	$[M+Na]^+$
Elements:		C (0-80); H (0-120); O (0-30); Na (0-5)			
Ion Formula		**Calculated m/z**		**PPM Error**	
C30H42NaO3		473.3026		-0.54	

Agilent Technologies

Figure S18 HRESIMS spectrum of compound **2** in MeOH.

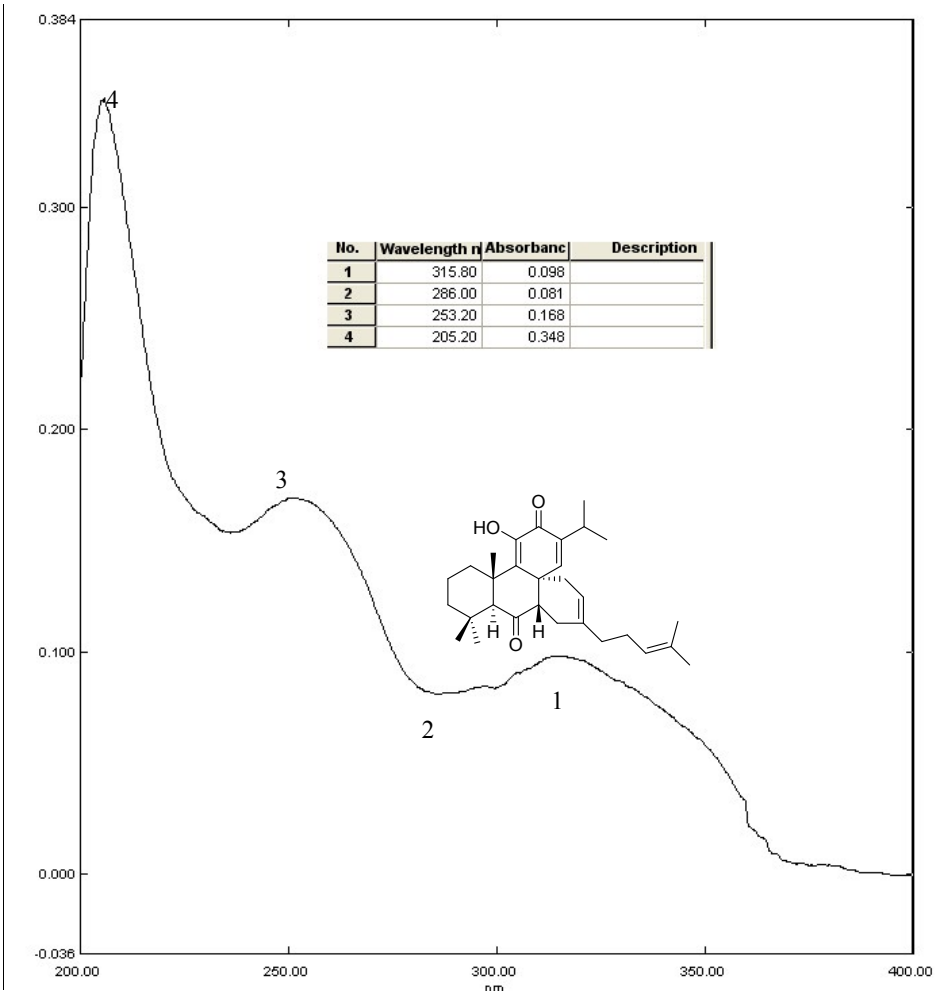

Figure S19 UV spectrum of compound **2** in MeOH.

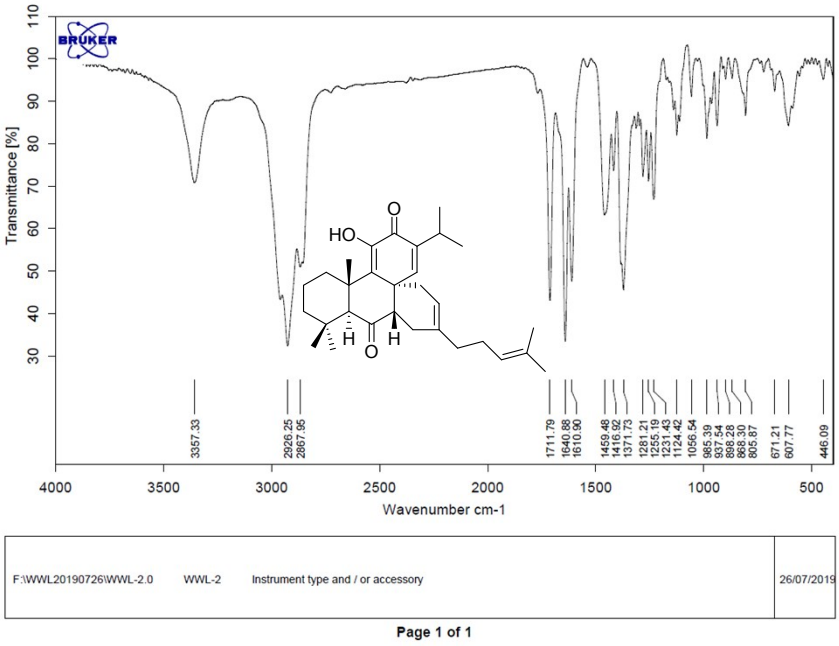

Figure S20 IR (KBr disc) spectrum of compound **2**.

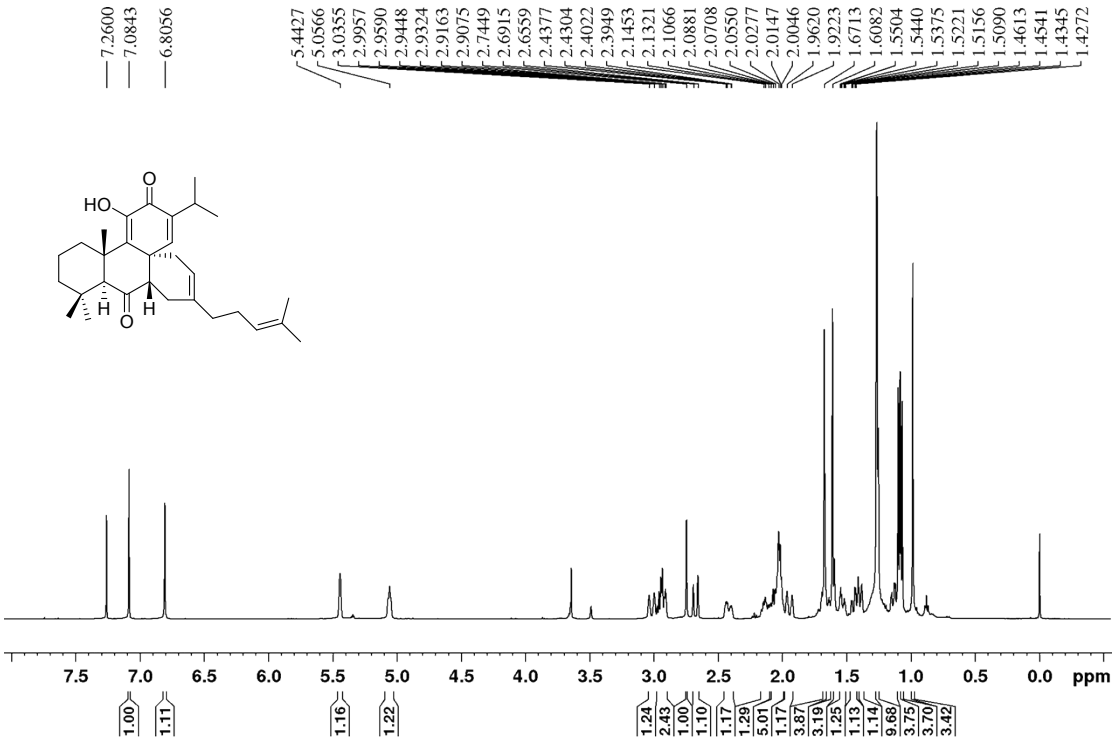

Figure S21 ^{1}H NMR spectrum of compound **2** in $CDCl_3$ (500 MHz).

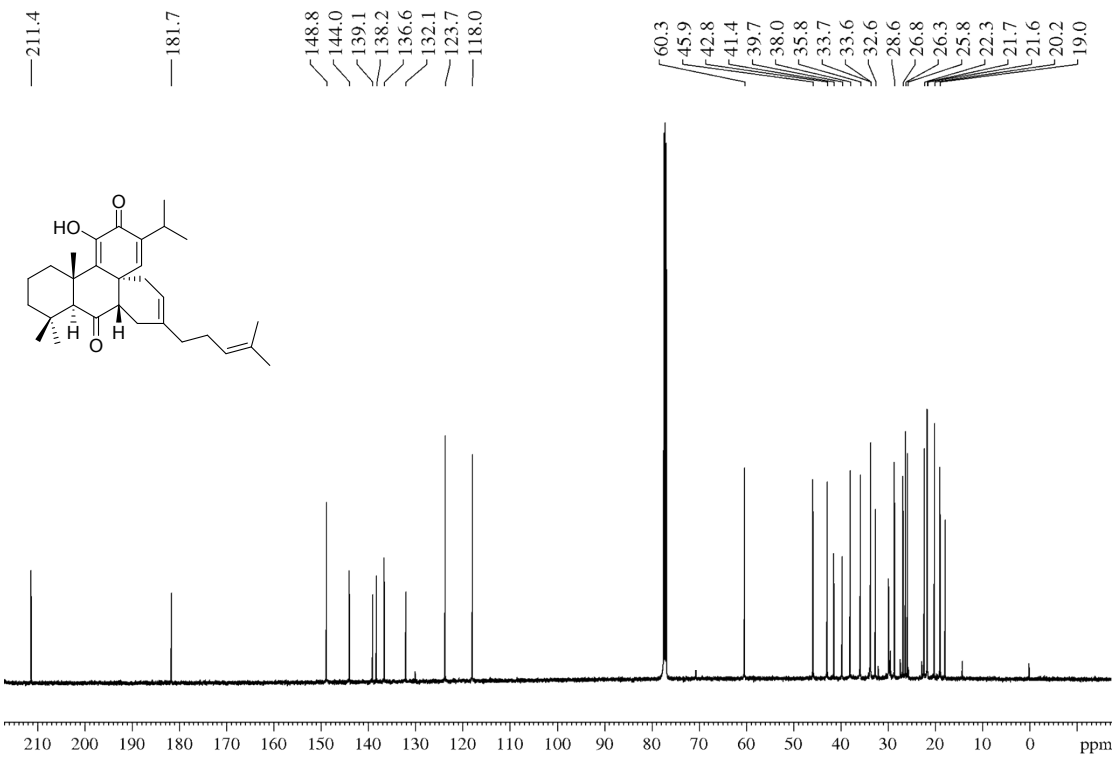

Figure S22 ^{13}C NMR spectrum of compound **2** in $CDCl_3$ (125 MHz).

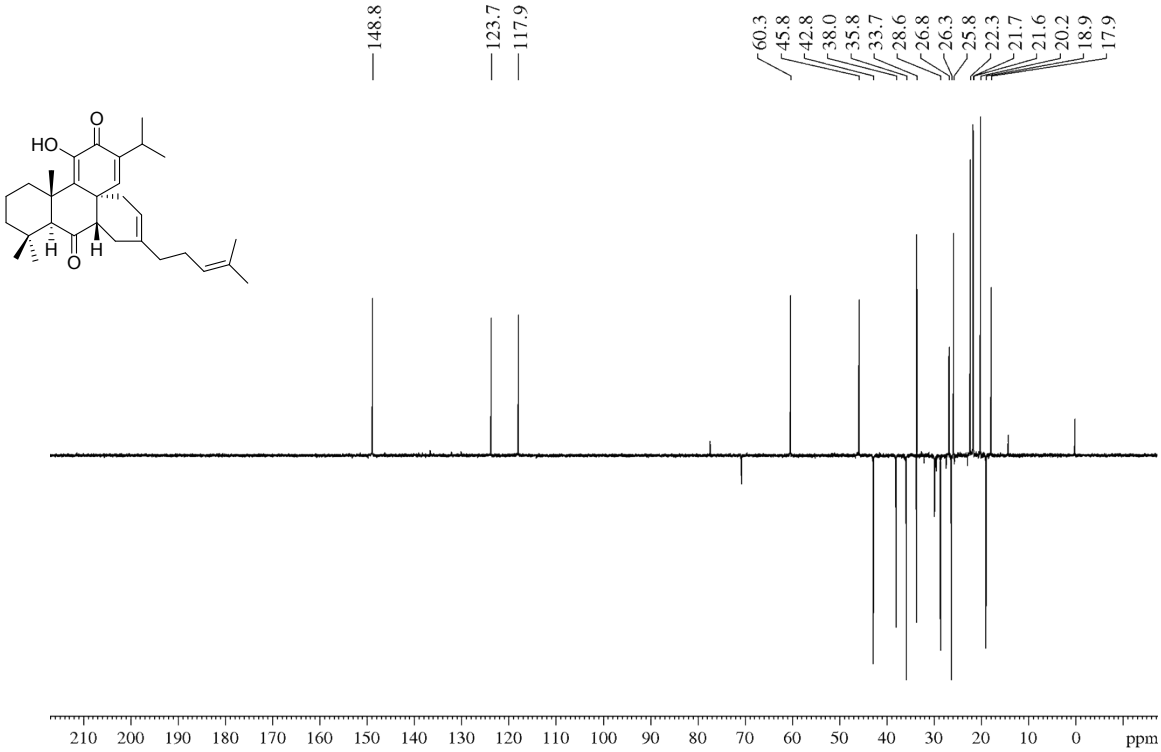

Figure S23 DEPT spectrum of compound **2** in $CDCl_3$ (150 MHz).

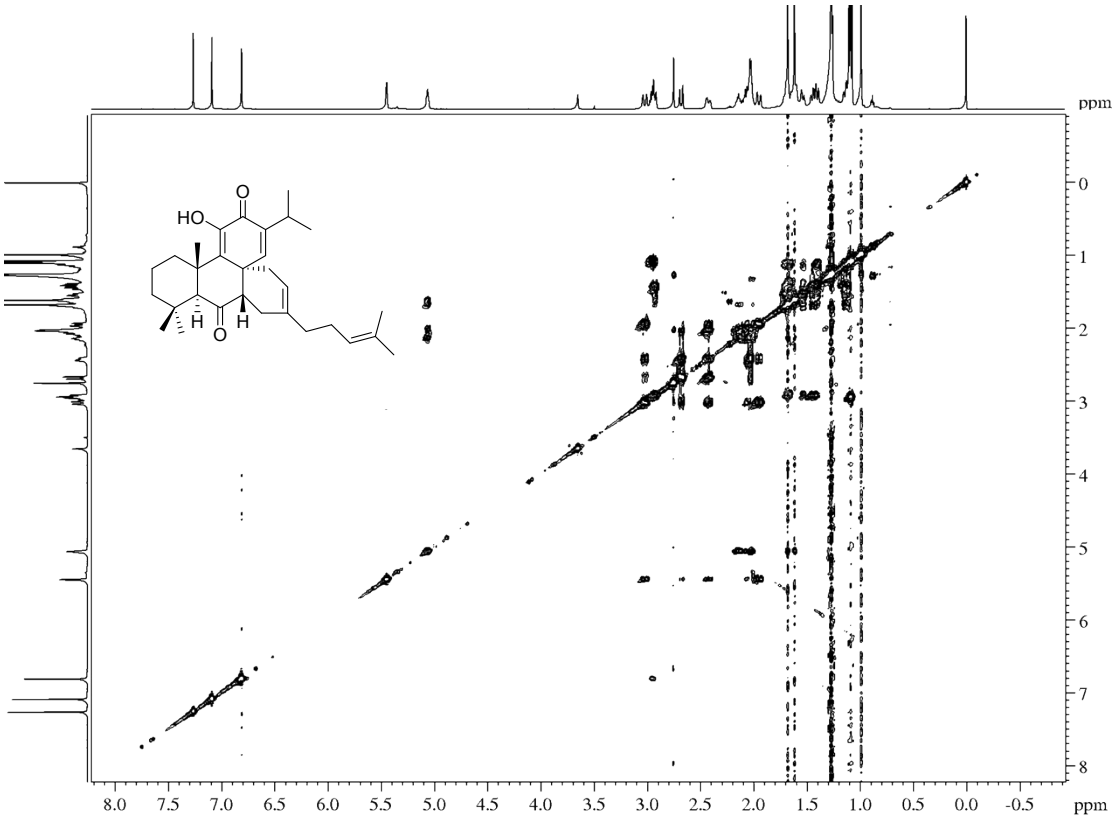

Figure S24 ^{1}H-^{1}H COSY spectrum of compound **2** in $CDCl_3$ (600 MHz).

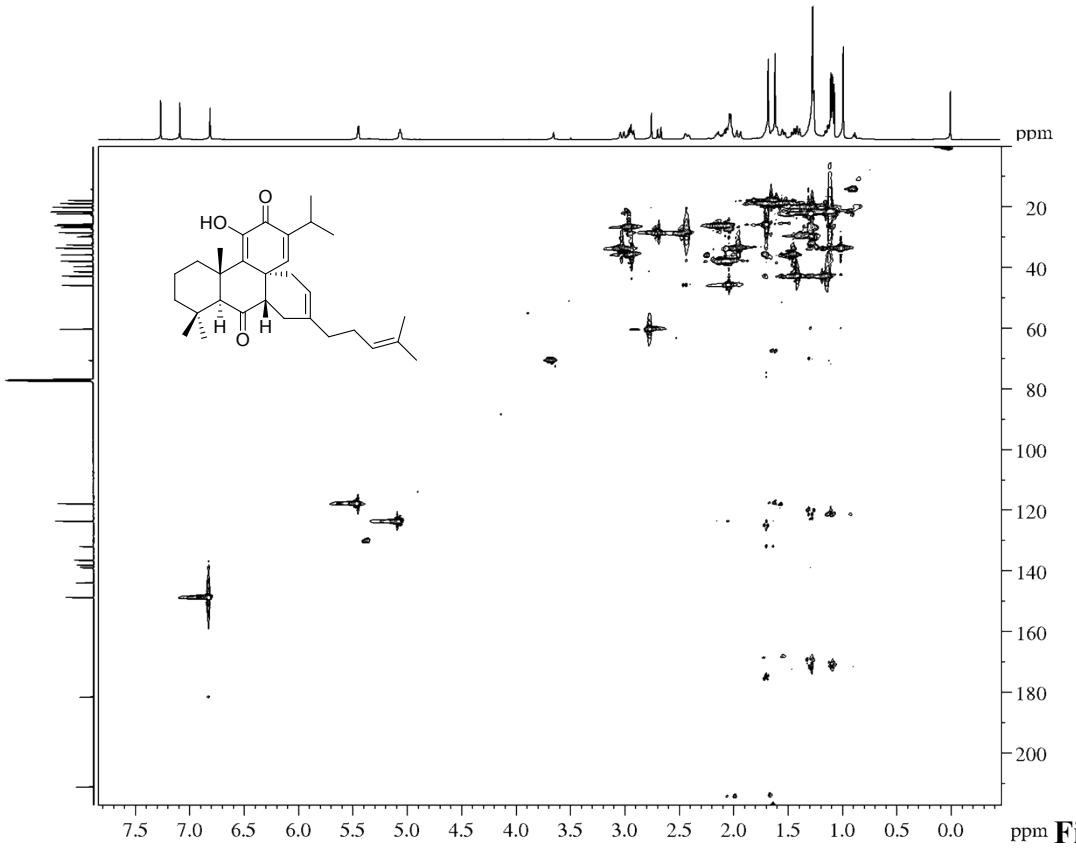

Figure S25 HSQC spectrum of compound **2** in $CDCl_3$ (600 MHz).

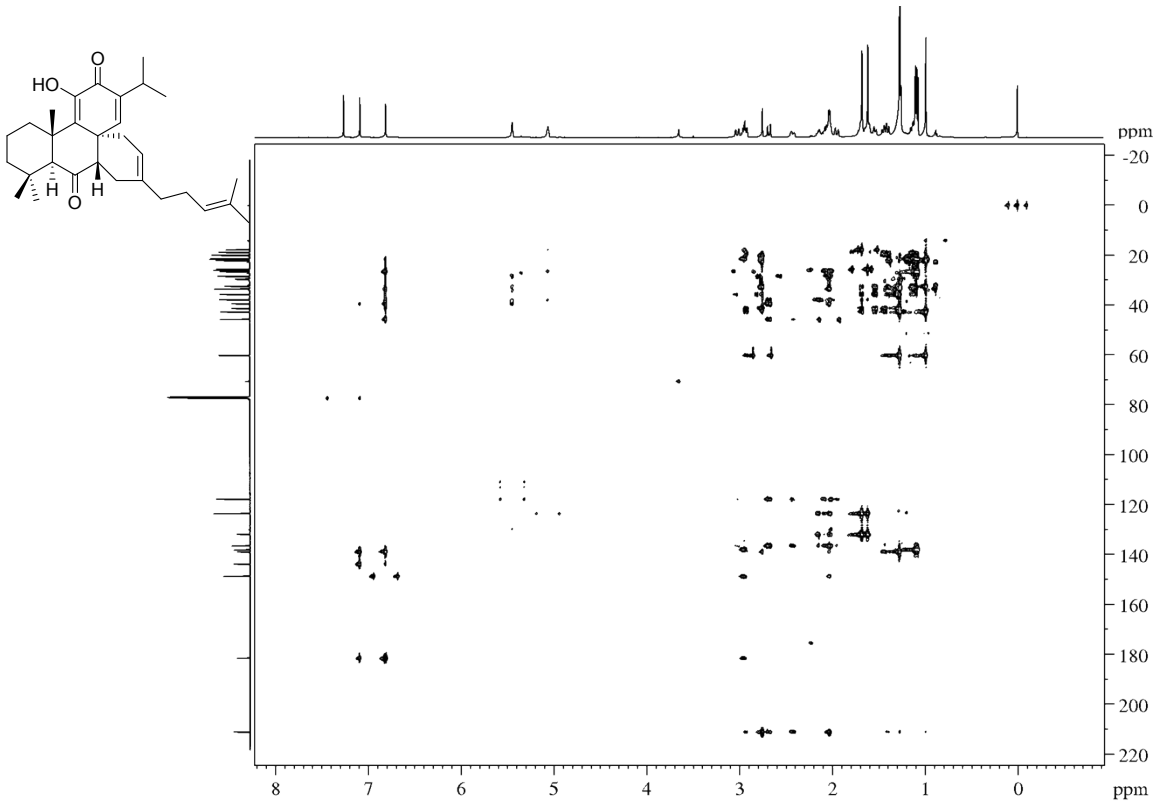

Figure S26 HMBC spectrum of compound **2** in $CDCl_3$ (600 MHz).

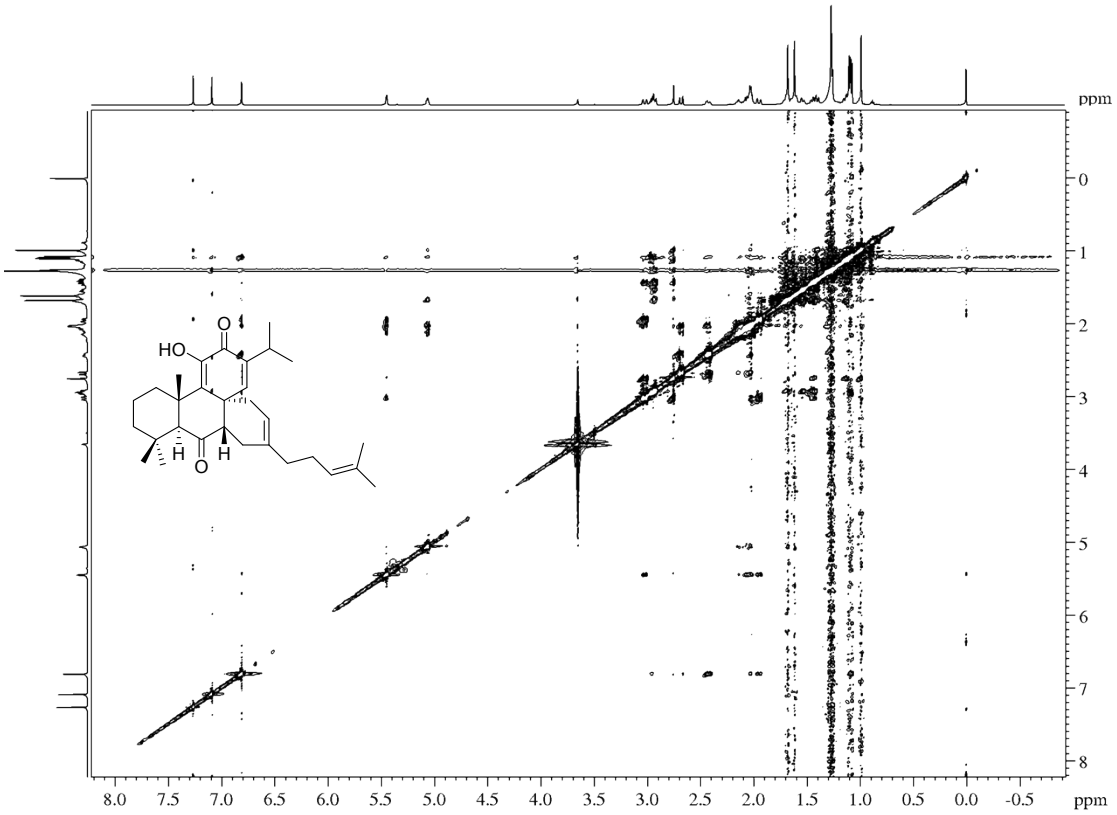

Figure S27 ROESY spectrum of compound **2** in $CDCl_3$ (600 MHz).

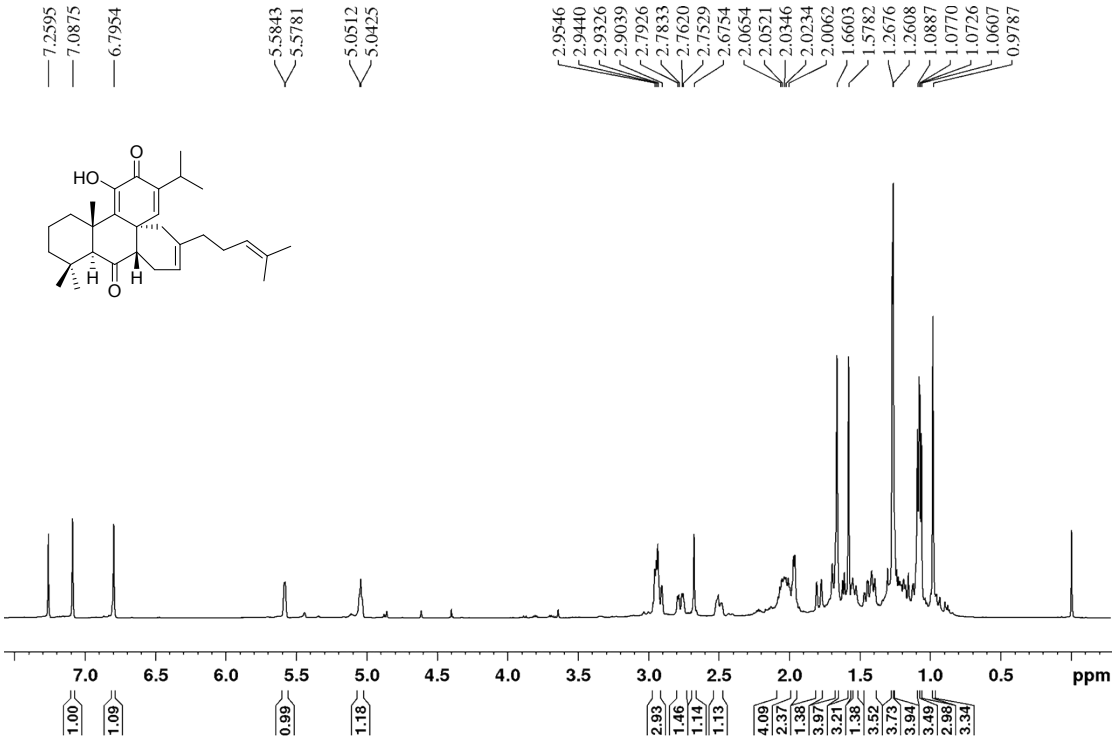

Figure S28 ^1H NMR spectrum of biomimetic synthesis of compound **1** in $CDCl_3$ (600 MHz).

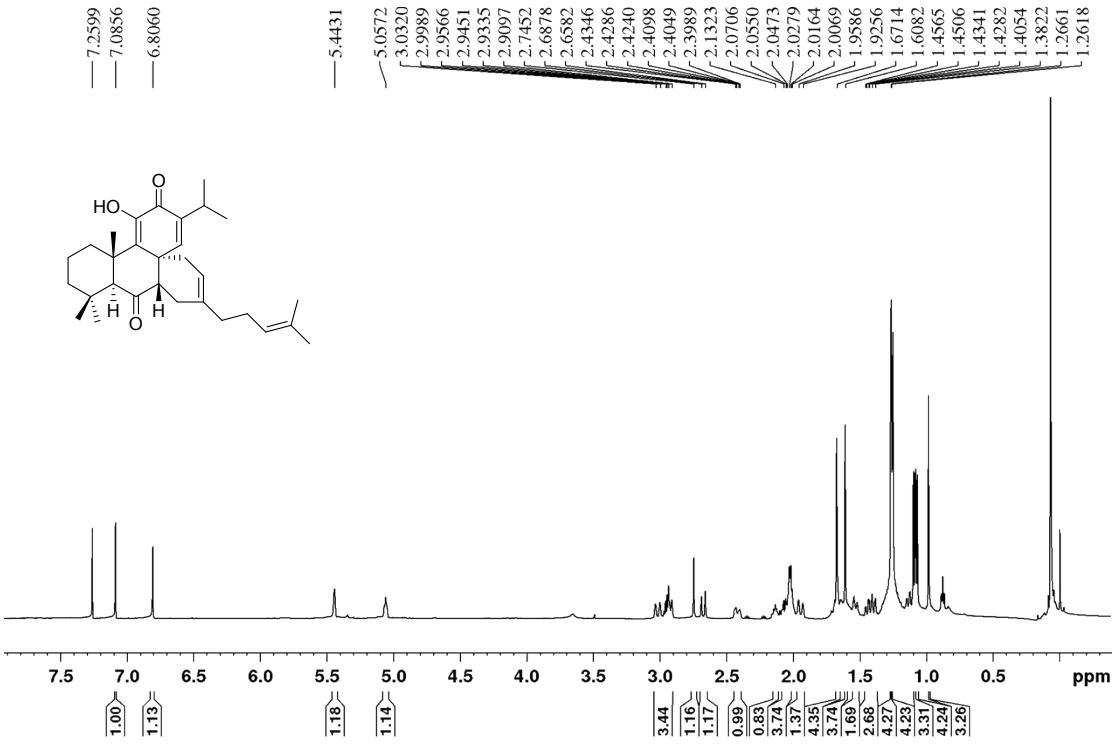

Figure S29 ^{1}H NMR spectrum of biomimetic synthesis of compound **2** in $CDCl_3$ (600 MHz).